Triple-Axis Tutorial Agenda
February 16, 2010

8:30	Coffee/Introductions
9:00	Welcome and Introduction (Jeff Lynn)
9:10	Triple-axis basics (Jeff Lynn)
	TAS technique
	Choice of Instrument
	Science examples
10:15	Break
10:30	Overview of triple-axis instruments at the NCNR (Songxue Chi)
	BT-7, BT-9, SPINS, MACS
10:45	Samples and Sample Environment—what you need (Deepak Singh)
	Elastic vs. Inelastic experiments
	Powders and single crystals
	Sample Environment equipment
11:00	Data Analysis—DAVE (William Ratcliff)
	Elastic scattering. Corrections to data
	Inelastic measurements. Corrections to data
	Planning tools
12:00	Lunch
12:58:30	Group Photo
1:00	Facility Tour—NCNR capabilities (Jeff Lynn and Sung Chang)
2:00	Hands-on data analysis: Elastic scattering example
	Magnetic structure and sublattice magnetization of $SrFe_2As_2$
3:15	Break
3:30	Hands-on data analysis: Inelastic scattering example
	Spin waves in the colossal magnetoresistive system $La_{0.7}Sr_{0.3}MnO_3$
4:45	Summary and discussion
5:00	Course completion

Contacts:	**Dr. Sung Chang**	**(301 975-8369)**	**Sung.Chang@nist.gov**
	Dr. Songxue Chi	**(301 975-4570)**	**Songxue.Chi@nist.gov**
	Dr. Jeffrey Lynn	**(301 975-6246)**	**Jeff.Lynn@nist.gov**
	Dr. William Ratcliff	**(301 975-4316)**	**William.Ratcliff@nist.gov**
	Dr. Deepak Singh	**(301 975-4863)**	**Deepak.Singh@nist.gov**

Choice of Spectrometer for Inelastic Scattering

Jeff Lynn

NCNR

Outline

- Inelastic Neutron Instrumentation
- Triple Axis Technique (crystal spectrometers)
- Science Examples
  - Colossal MagnetoResistive (CMR) systems
    - Spin Waves
    - Polarons
  - Phonon dispersion & Density of States
  - Superconductors
    - Cuprates
    - Iron-based superconductors
  - Multiferroics (Magnetic Ferroelectrics)

Inelastic Spectrometers

Thermal triple-axis instruments
BT-7 and BT-9

Cold neutron triple-axis instrument
(SPINS and MACS)

Filter analyzer spectrometer (FANS)

High flux backscattering spectrometer (HFBS)

Disk chopper time-of-flight spectrometer (DCS)

Spin-echo spectrometer

Neutron Dispersion Relation

$$E_{neutron} = \left(\frac{p^2}{2m}\right) = \left(\frac{\hbar^2 k^2}{2m}\right) = 2.07\,k^2 = \left(\frac{h^2}{2m\lambda^2}\right) = 81.8/\lambda^2$$

$$p = \hbar k \qquad k = 2\pi/\lambda$$

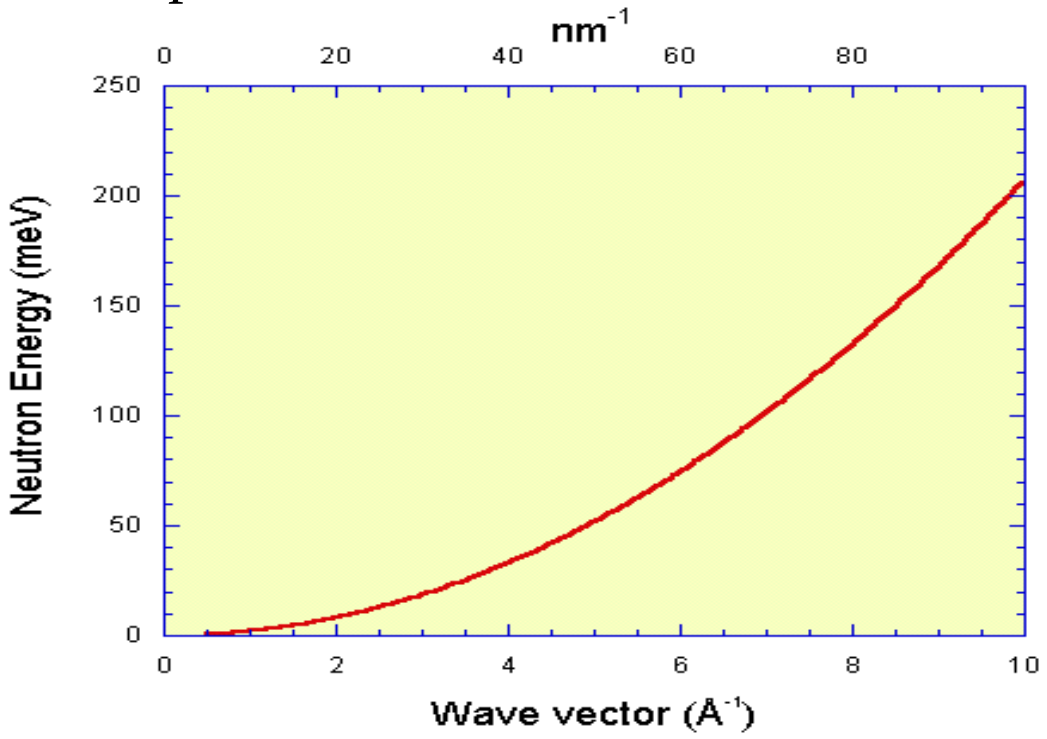

Other Probes

$$E_{photon}\ (keV) = 2.0\,k = 12.4 / \lambda$$

$$E_{electron}\ (eV) = 3.8\,k^2 = 150 / \lambda^2$$

1.54 Å corresponds to

X-ray: $9.3 \cdot 10^7$ K

Electron: $7.4 \cdot 10^5$ K

Neutron: 400 K

$$1\ meV = 11.6\ K \quad (k_B T)$$

$$1\ meV = 8.06\ cm^{-1} \quad (E / hc)$$

$$1\ meV = 0.24\ THz \quad (E / h)$$

$$1\ meV / \mu_B = 17.3\ T \quad (E / \mu_B)$$

Conservation of Momentum and Energy

$$\mathbf{Q} = \mathbf{k}_i - \mathbf{k}_f$$

$$\Delta E = \frac{\hbar^2 k_i^2}{2m} - \frac{\hbar^2 k_f^2}{2m}$$

$$\mathbf{Q}_C = \tau + \mathbf{q}$$

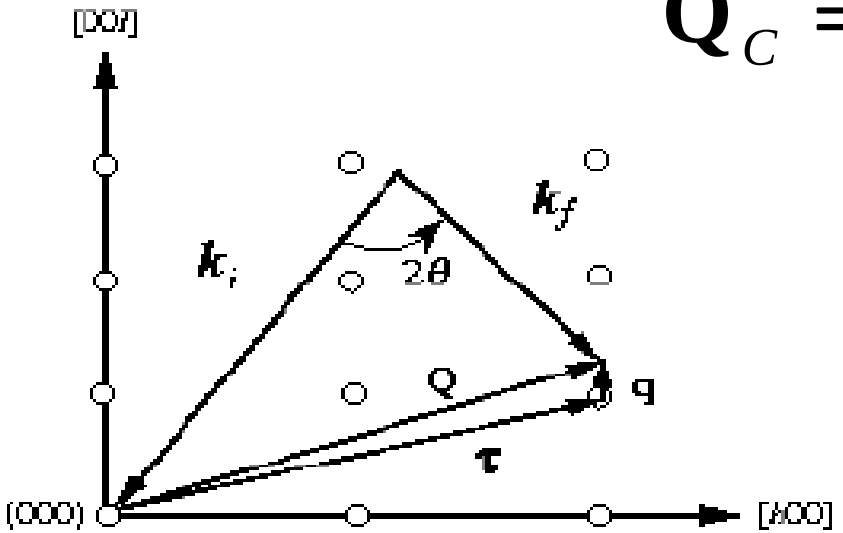

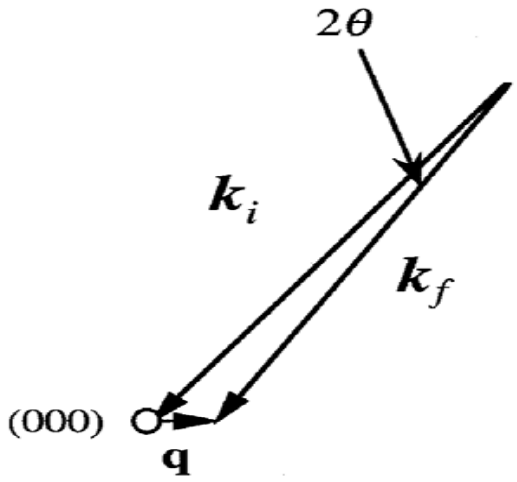

Reciprocal Space for Thermal Neutrons

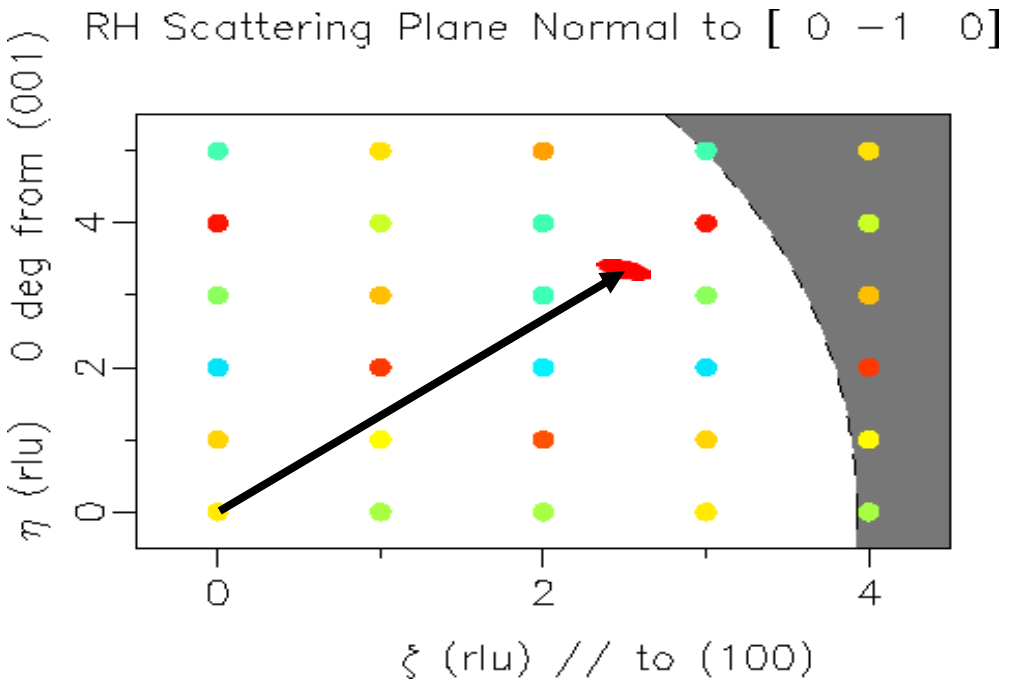

Reciprocal Space for Powder

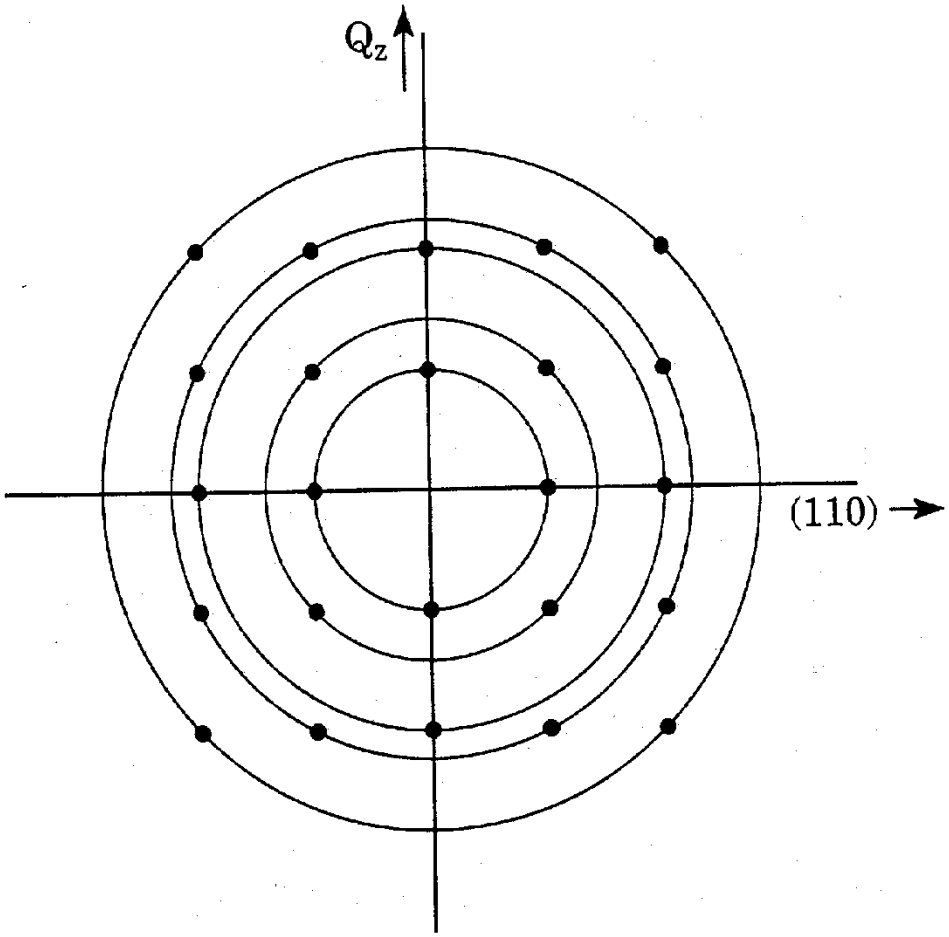

Triple-Axis Spectrometer

$$\lambda_i = 2 d_M \sin(\theta_M)$$

$$\lambda_f = 2 d_A \sin(\theta_A)$$

$$\Delta\lambda = 2 d_M \cos(\theta_M) \Delta\theta_M$$

$$\Delta E = \frac{\hbar^2 k_i^2}{2m} - \frac{\hbar^2 k_f^2}{2m}$$

$$k = 2\pi / \lambda$$

Conventional Triple-Axis Spectroscopy (TAS)

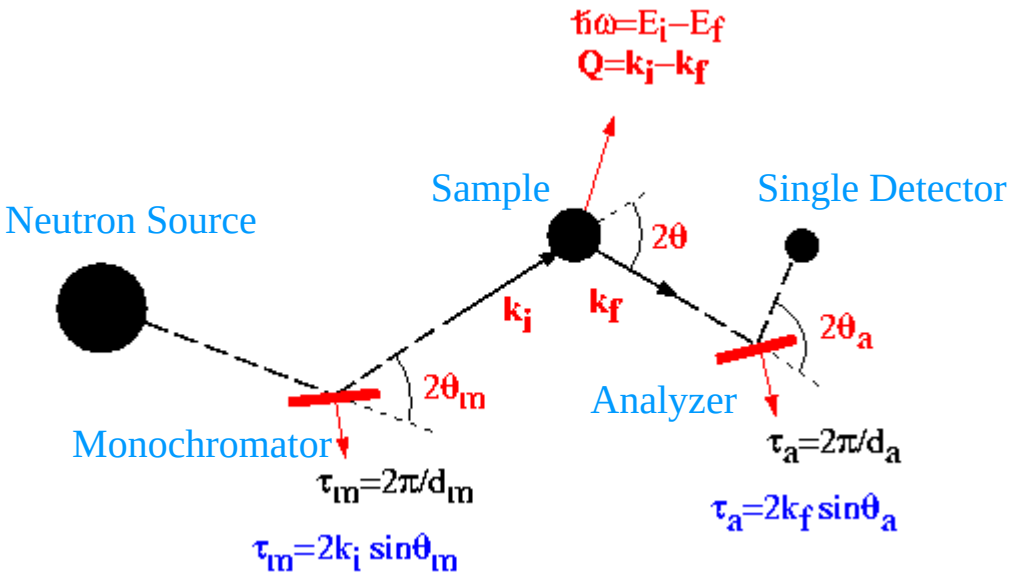

A single point at a time

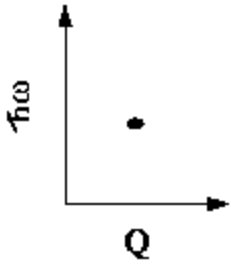

TAS is ideally suited for probing small regions of phase space

Shortcoming: Low data collection rate

High Energy Resolution

- $E = C/(2\pi/\lambda)^2$
- $\Delta E = C' / \lambda^3$
- Cold Neutrons Needed

Reciprocal Space for Thermal & Cold Neutrons

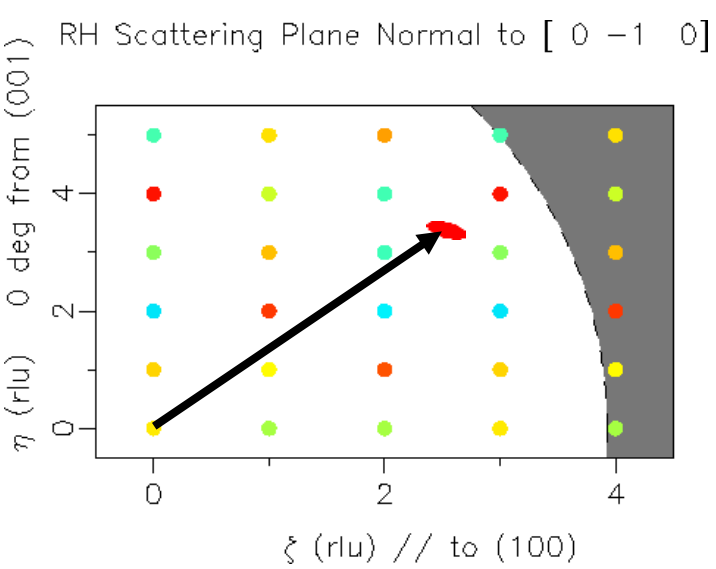

Thermal

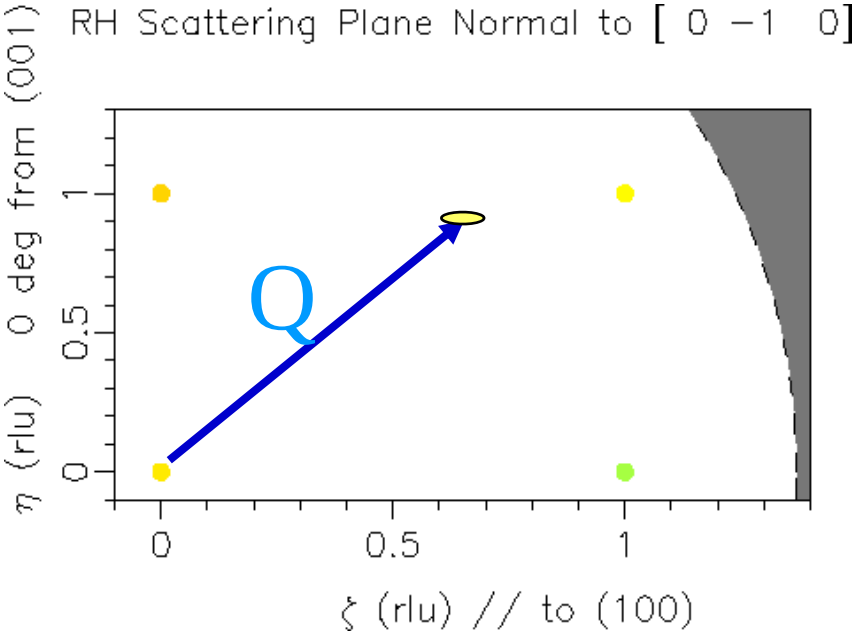

Cold

Magnons and Phonons

$$\left(\frac{d^2\sigma}{d\Omega dE_f}\right)^{\pm} = \left(\frac{\gamma e^2}{2mc^2}\right)^2 \frac{k_f}{k_i} f(Q)^2 \mu_z \left(n_q + \tfrac{1}{2} \pm \tfrac{1}{2}\right) \delta\left(\hbar\omega \mp \hbar\omega_q\right) \times \delta\left(\mathbf{Q} \mp \mathbf{q} - \boldsymbol{\tau}\cdot\right) \left\{1 + \left(\hat{\mathbf{Q}}\cdot\hat{\boldsymbol{\eta}}\right)^2 \mp 2\left(\hat{\mathbf{P}}\cdot\hat{\mathbf{Q}}\right)\left(\hat{\mathbf{Q}}\cdot\hat{\boldsymbol{\eta}}\right)\right\}$$

Magnons

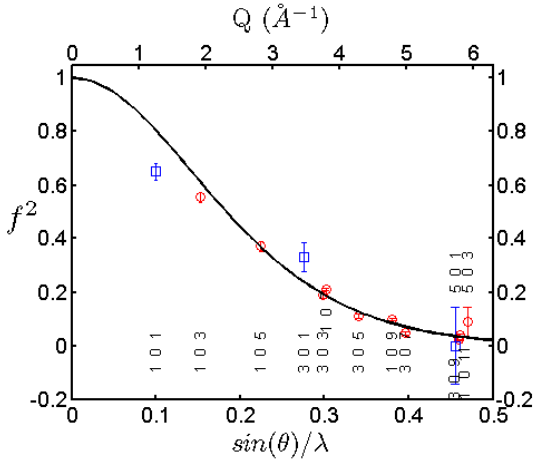

$$\left(\frac{d^2\sigma}{d\Omega dE_f}\right)^{\pm} = \sigma_c c \left|Q\cdot\varepsilon\right|^2 \frac{n(E/kT)}{m\omega_q} \ldots$$

Phonons

Reciprocal Space for Thermal & Cold Neutrons

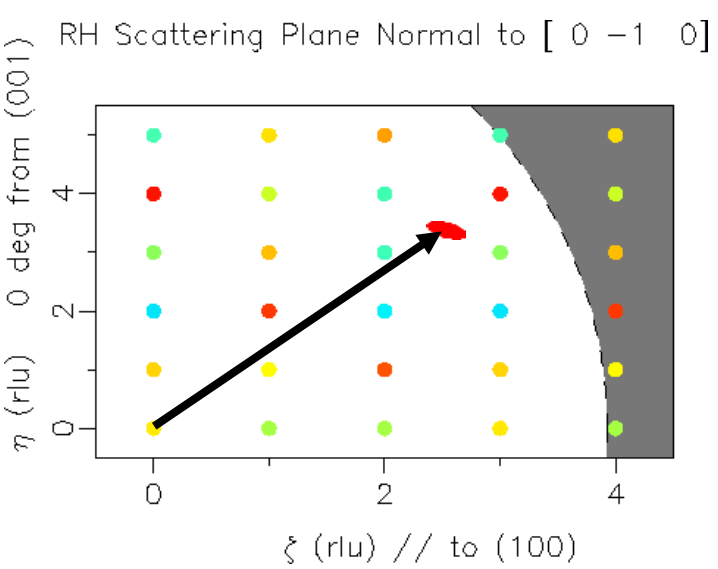

Thermal

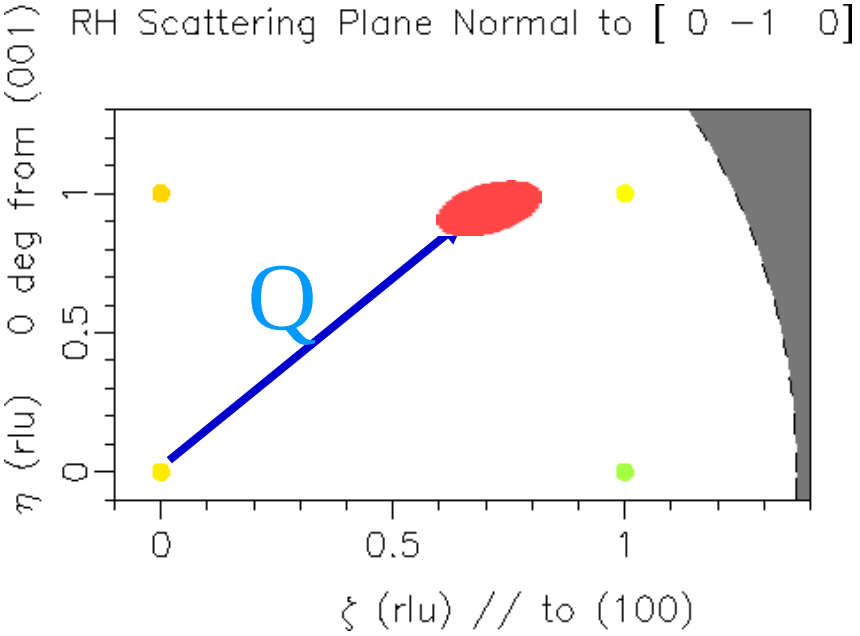

Cold

Conventional Triple-Axis Spectroscopy (TAS)

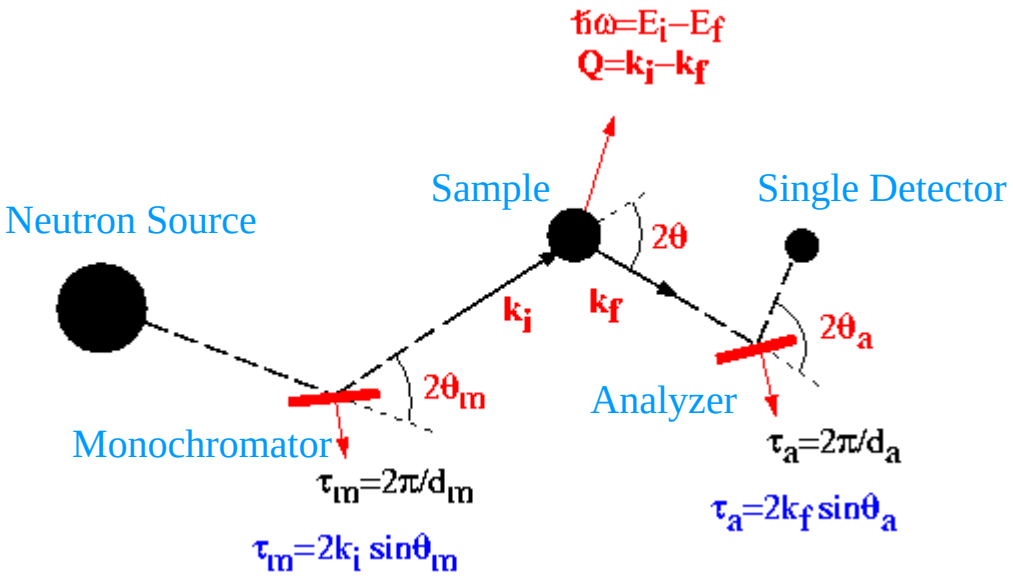

A single point at a time

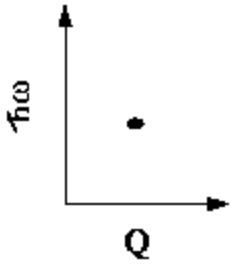

TAS is ideally suited for probing small regions of phase space

Shortcoming: Low data collection rate

Improvement

Multicrystal analyzer and position-sensitive detector

Horizontally Focusing (HF) Analyzer Mode

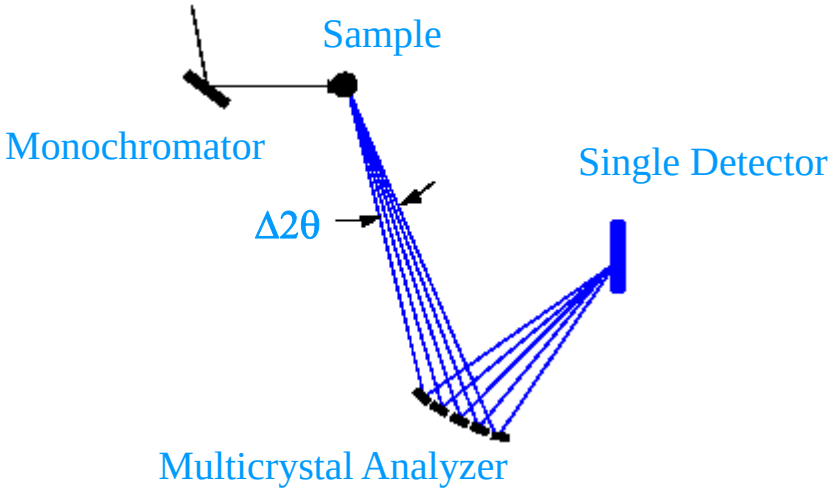

Relaxed Q-resolution

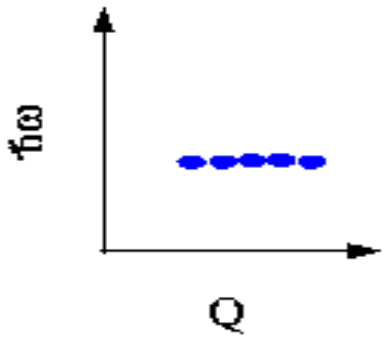

L = distance from sample to HF analyzer
w_a = total width of HF analyzer

$\Delta 2\theta = w_a \sin\theta_a / L \sim 9$ degree for E_f=5 meV at SPINS

Useful for studying systems with short-range correlations

Position-Sensitive Detector Mode

with Flat Analyzer (not focusing)

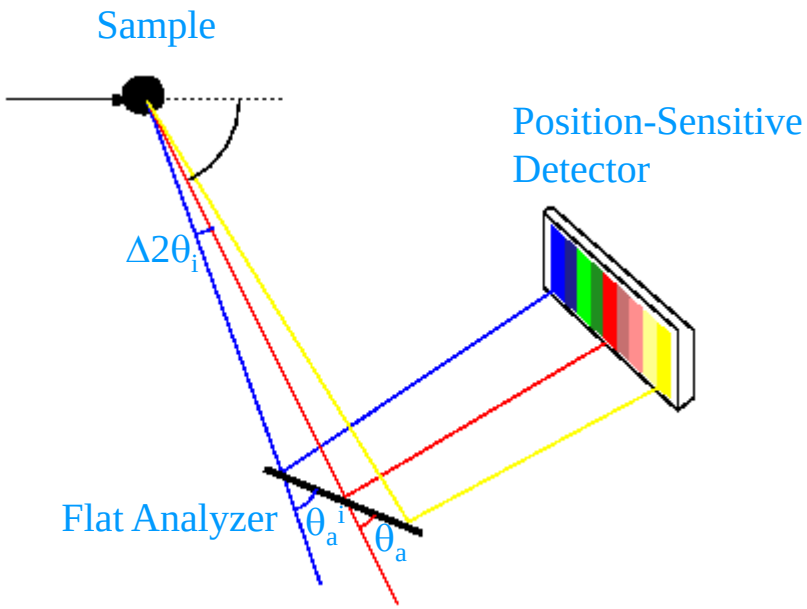

$\theta_a^i = \theta_a + \Delta 2\theta_i = \theta_a - \text{atan}(x \sin\theta_a/(L+x\cos\theta_a))$

$k_f^i = \tau_a/2\sin\theta_a^i$

$\mathbf{Q_i = k_i - k_f^i}$

Good Q-resolution

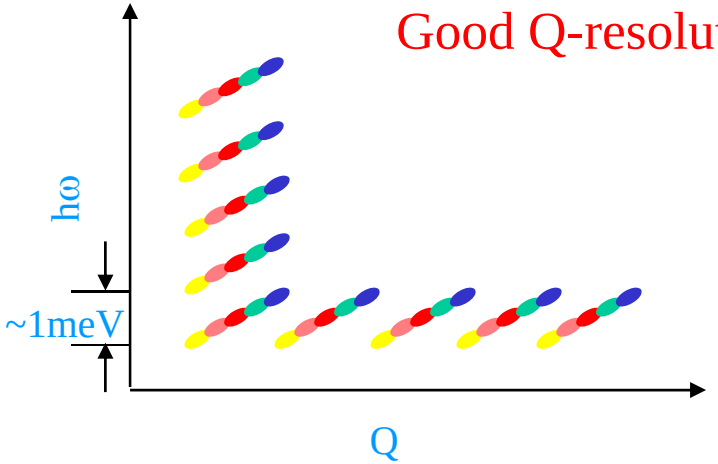

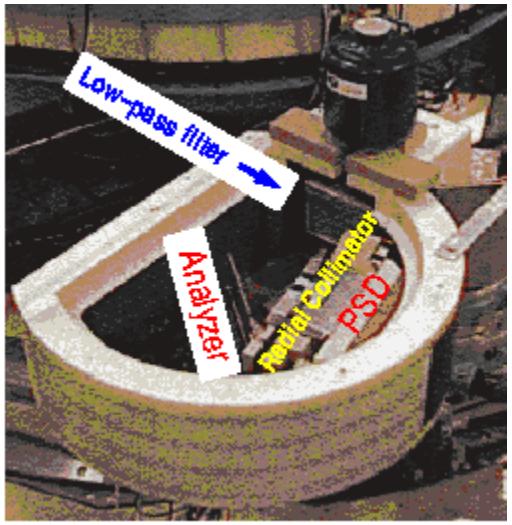

Probes scattering events at different energy and momentum transfers simultaneously

Survey (hω-Q) space by changing the incident energy and scattering angle

Multiple Detectors

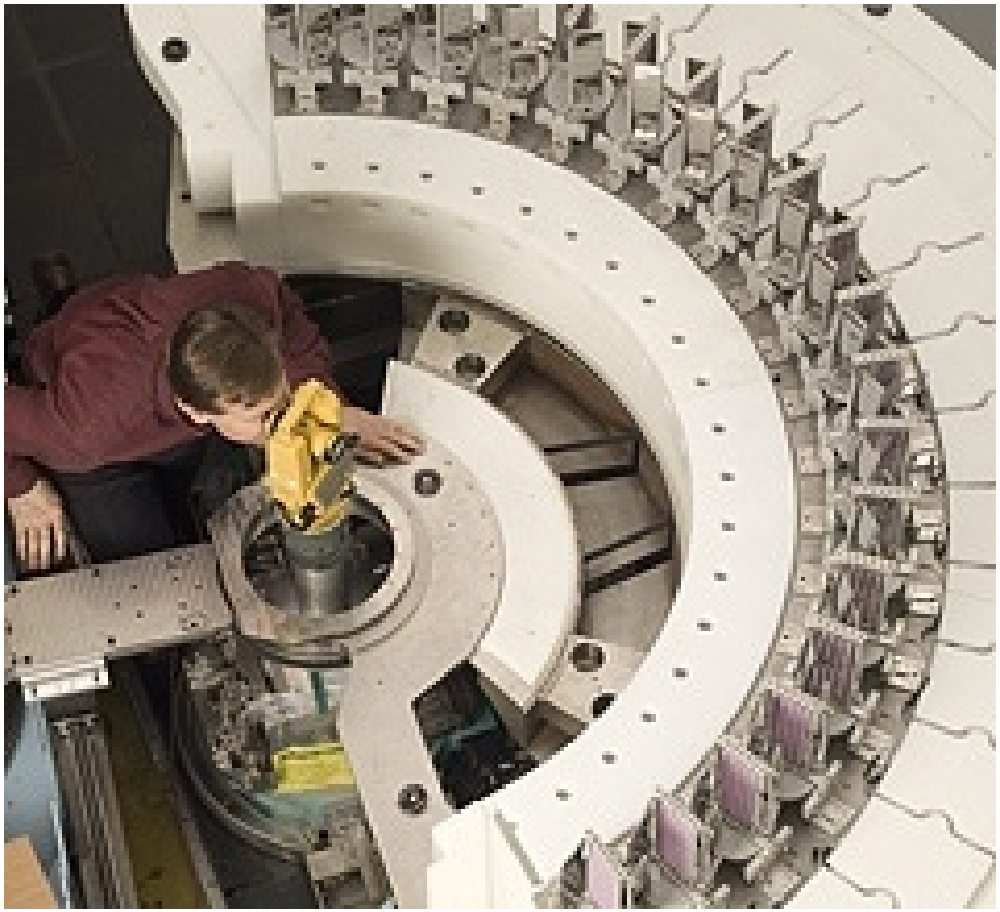

BT-7 New Thermal TAS

Overview

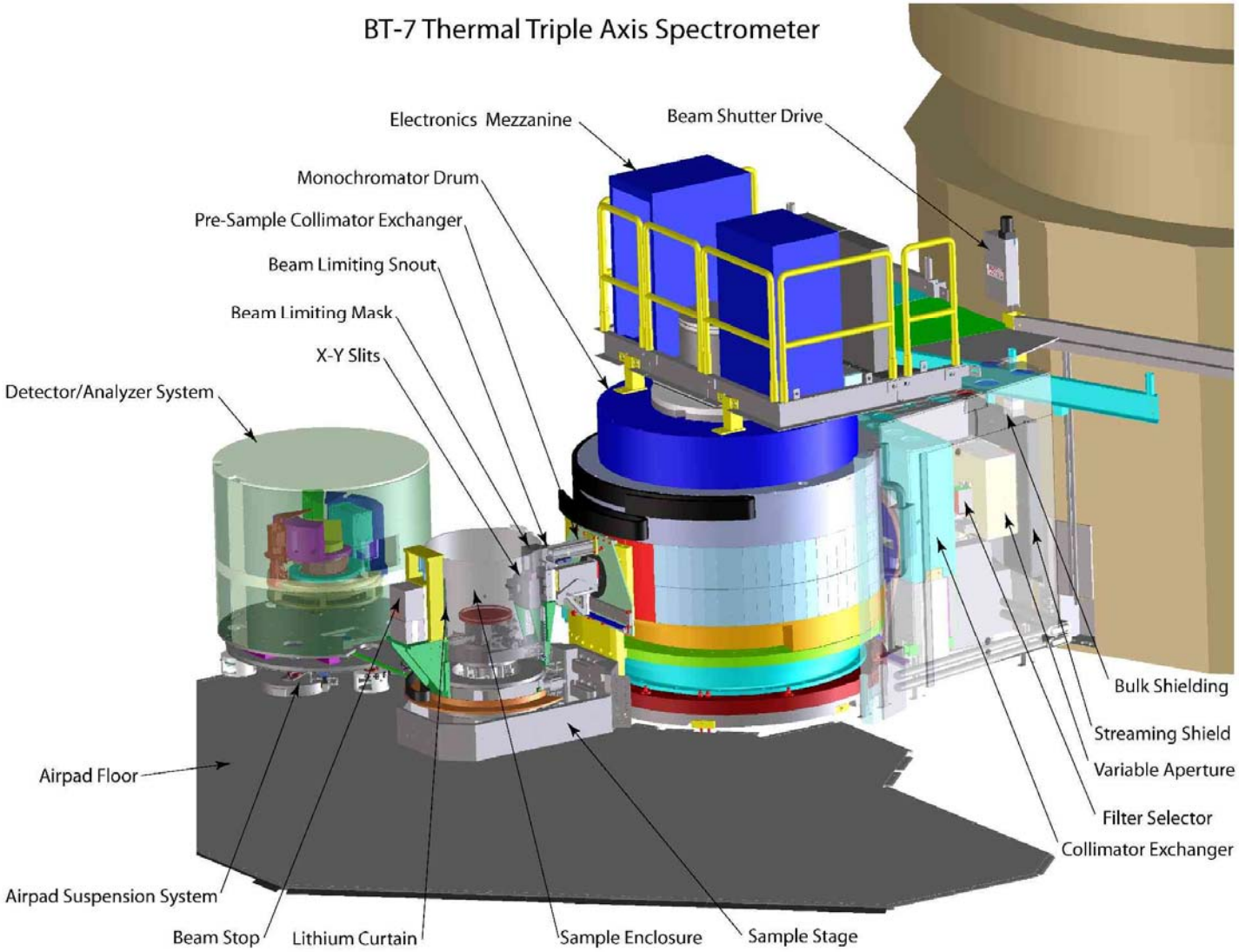

Features

- Make full use of reactor beam (ID=15 cm)
- Choice of Monochromators (3 → 2)
- Polarized Beam (Heusler→He^3)
- Elevator, magnet axis for sample
- Interchangeable Analyser Systems
  - Conventional
  - Horizontal Focusing
  - Flat PG + PSD
  - Diffraction with PSD
- Multicrystal/detector Array
- Double Focusing

Double focusing monochromators

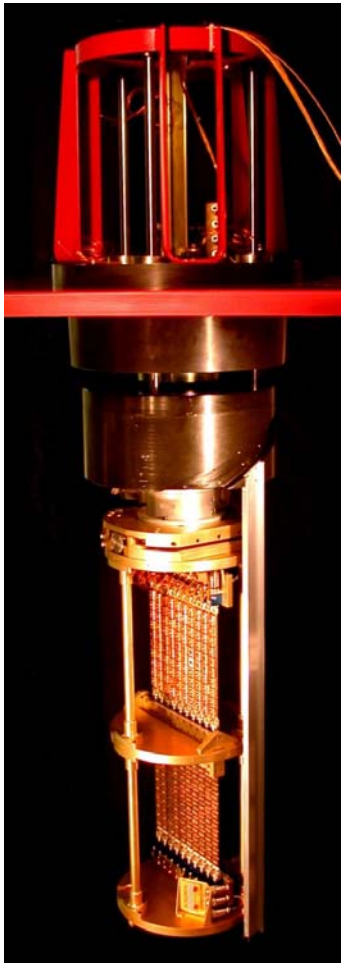

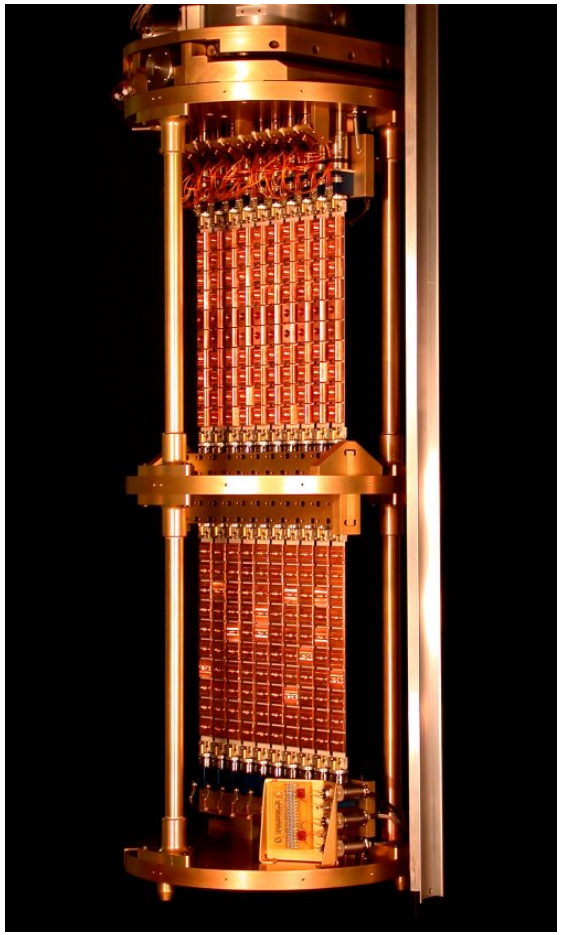

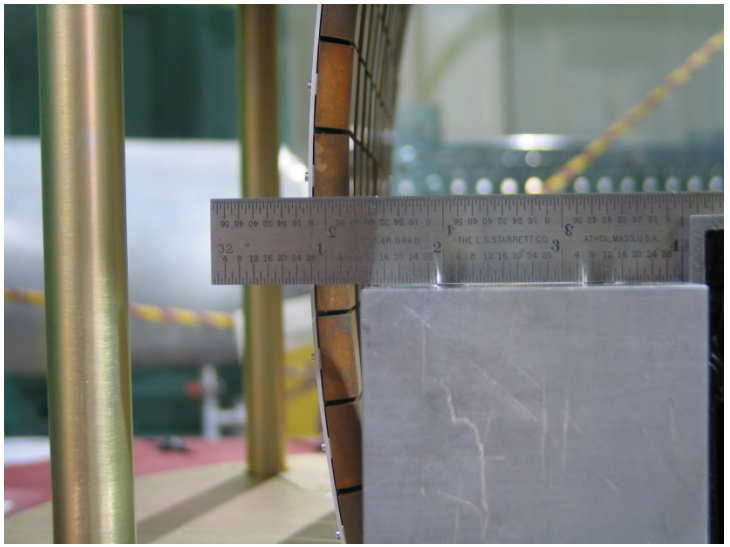

PG(002) d = 3.35 Å

Cu(220) d = 1.27 Å

Monochromator Arrays

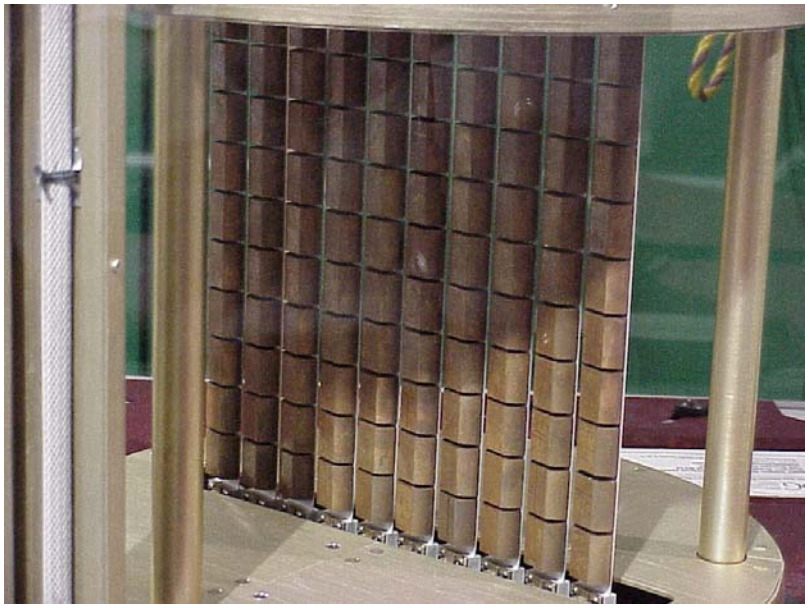

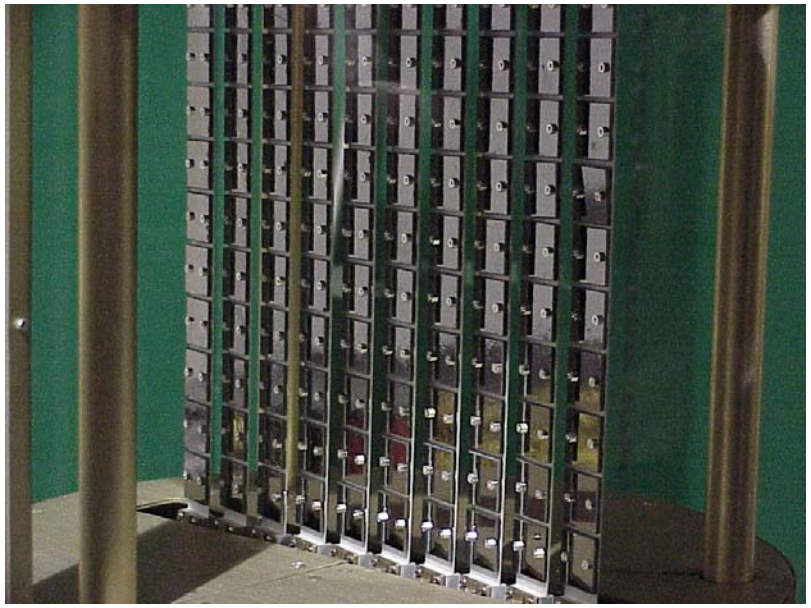

Cu(220) d = 1.27 Å PG(002) d = 3.35 Å

Monochromator Improvements

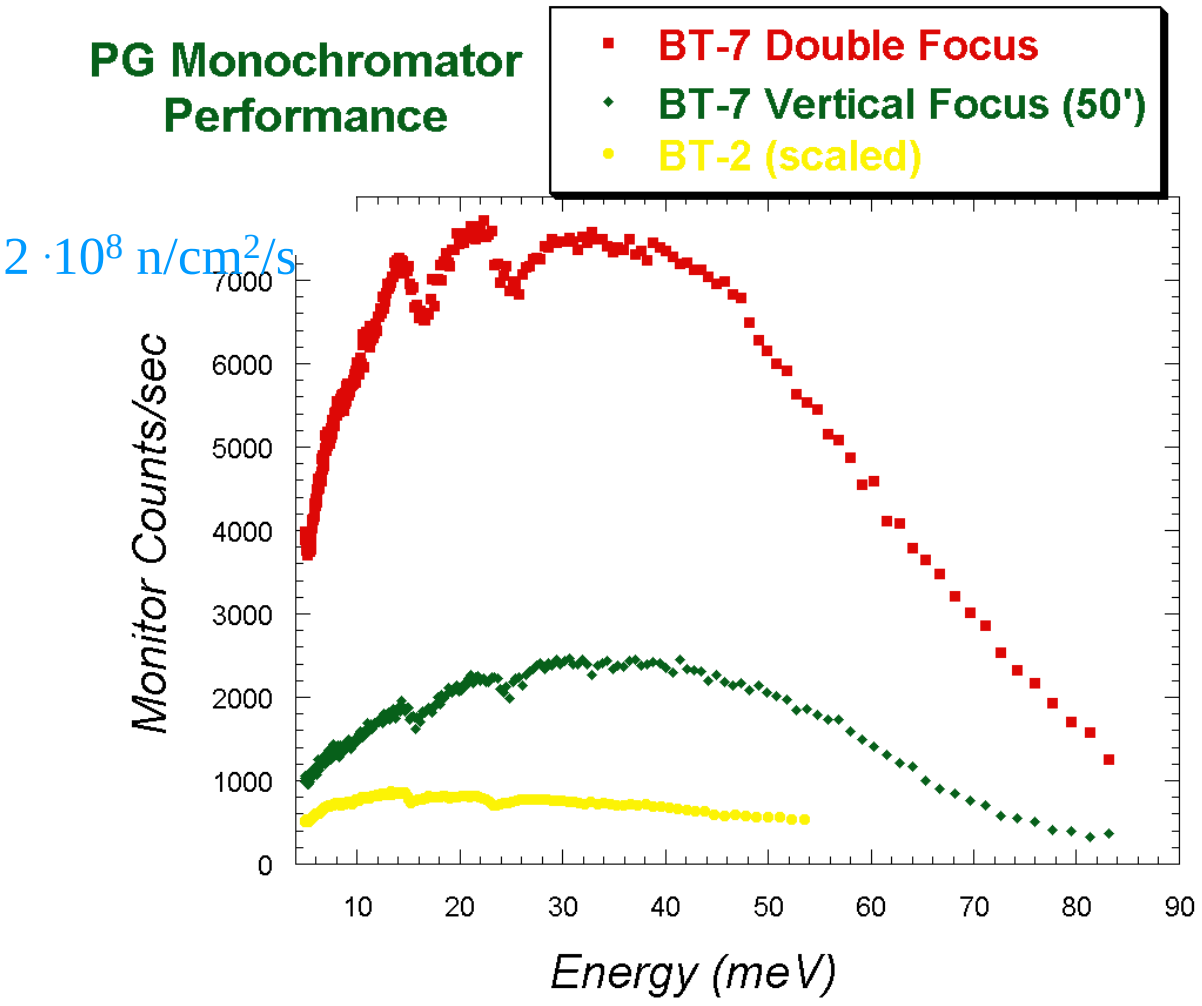

With vertical focusing, gain of 2.3 over BT-2/9 at 14.7 meV; gain of 3.5 at 40 meV.

Double focusing, gain of 8.7 at 14.7 meV; gain of 10.8 at 40 meV

Analyzer Modes

- Diffraction detector (single detector)
- Diffraction mode (radial collimator +PSD)
  - (door detector; poor man's PSD)
- Flat PG analyzer + collimation + SD
- Flat PG analyzer + PSD (range of **Q**, E or range of diffuse scatt.)
- Horizontal focusing (radial collimator + single detector)

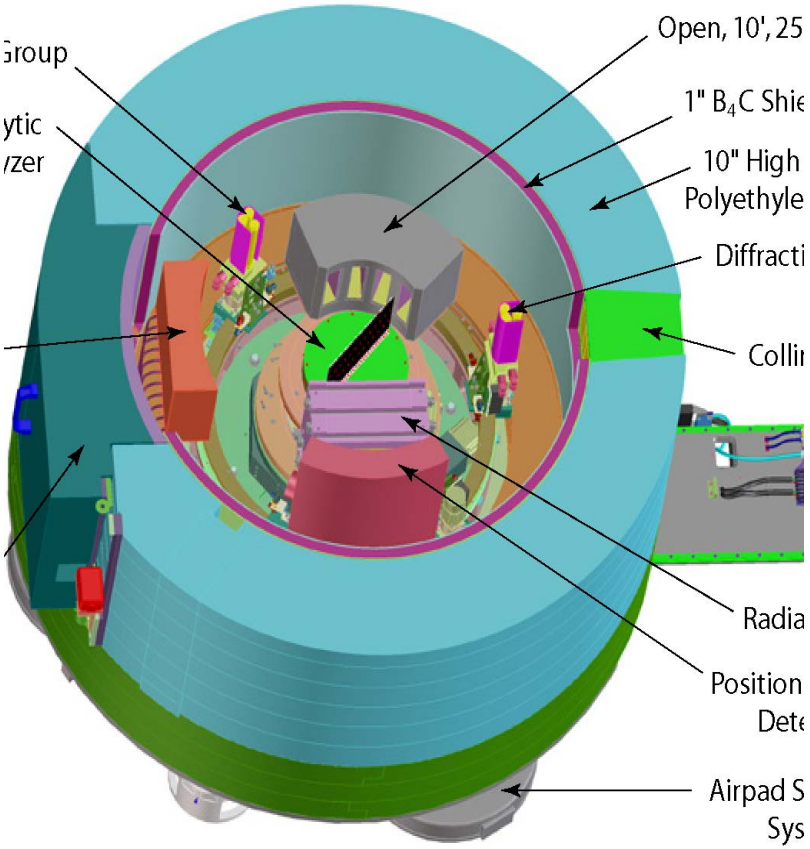

Filter Analyzer Spectrometer (FANS)

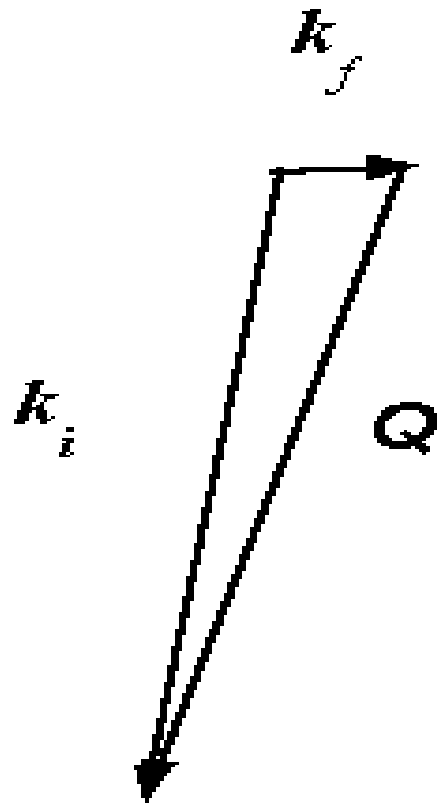

Perfect Resolution
Backscattering

$$\lambda_i = 2 d_M \sin(\theta_M)$$

$$\Delta\lambda = 2 d_M \cos(\theta_M) \Delta\theta_M$$

Thermal TA	1,000 μeV
Cold TA	100 μeV
HFBS	1 μeV

Spin Echo Spectrometer

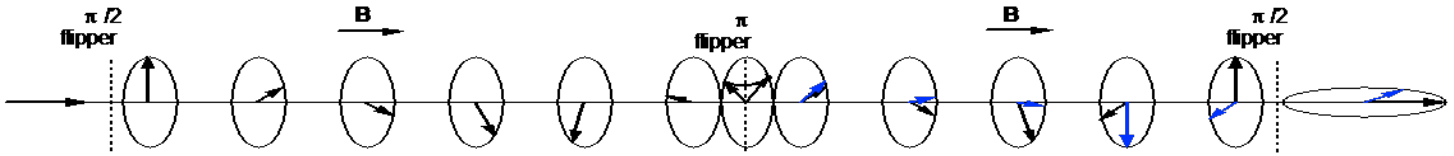

$$t = \frac{L}{v}$$

$$\phi = \omega t = \frac{\gamma BL}{v}$$

Inelastic Spectrometers

Triple-axis instruments

Filter analyzer spectrometer (FANS)

High flux backscattering spectrometer (HFBS)

Time-of-flight spectrometer (DCS)

Spin-echo spectrometer

NCNR

Time-of-flight Spectrometer

- Dynamics of systems where the excitations depend only on the magnitude of **Q**, and not its direction
- Phonon Density of States
- Excitations in randomized systems (glasses, liquids, …)
- Ionic diffusion
- Spin Diffusion
- Molecular vibrations
- Crystal field levels
- Tunneling

NIST Center for Neutron Research

NCNR

Facilities

Structure: Diffraction (2); SANS (3+1); Reflectometry (3)

Dynamics: TAS (5+1); TOF (1); Spin Echo (1)

Prompt-γ (2); Depth Profile (1); Topography (2); Activation Analysis; Fundamental Properties (3)--Interferometry

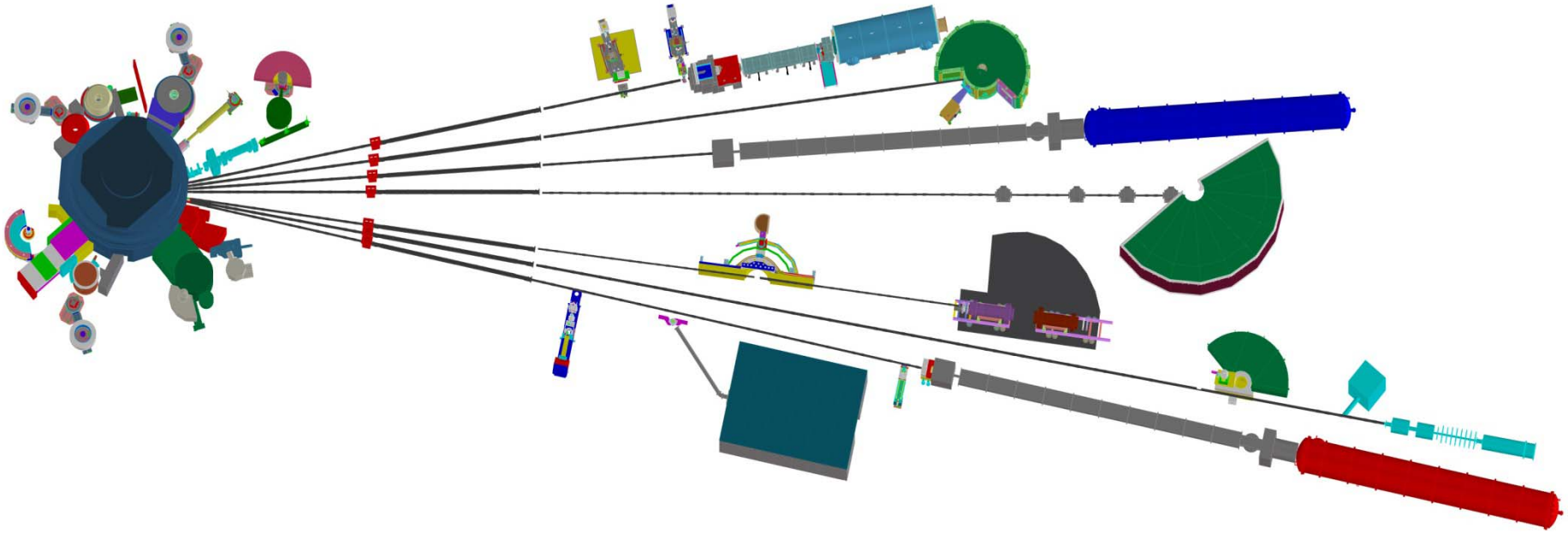

http://www.ncnr.nist.gov

Neutron Scattering Techniques

Diffraction

- **Crystallography**–powder, single crystal
  Atomic positions, lattice parameters, bond distances, mean-square vibrations as a function of T, H, P
- **Magnetism**
  Magnetic structure, order parameter, spin directions, spin density distribution
  Phase Transitions and Critical Phenomena (Scaling, Universality)
- **Small Angle Neutron Scattering (SANS)**
  Magnetic Correlation Length, Vortex Structures, Domain Structures, Grain boundaries, twin boundaries, defect structures
- **Thin Film Reflectometry**
  Density profiles, Magnetic structures, Magnetization profiles, Surface and Interface properties (flatness, roughness)

Inelastic Scattering

Lattice Dynamics

Phonon Density of States
Interatomic Force constants
Mean-square vibrations
Diffusion

Spin Dynamics

Exchange interactions
Magnetic Anisotropy
Magnetic Fluctuation Behavior
Crystal Field Levels
Magnetic-Structural Coupling

NCNR

Dynamic Range

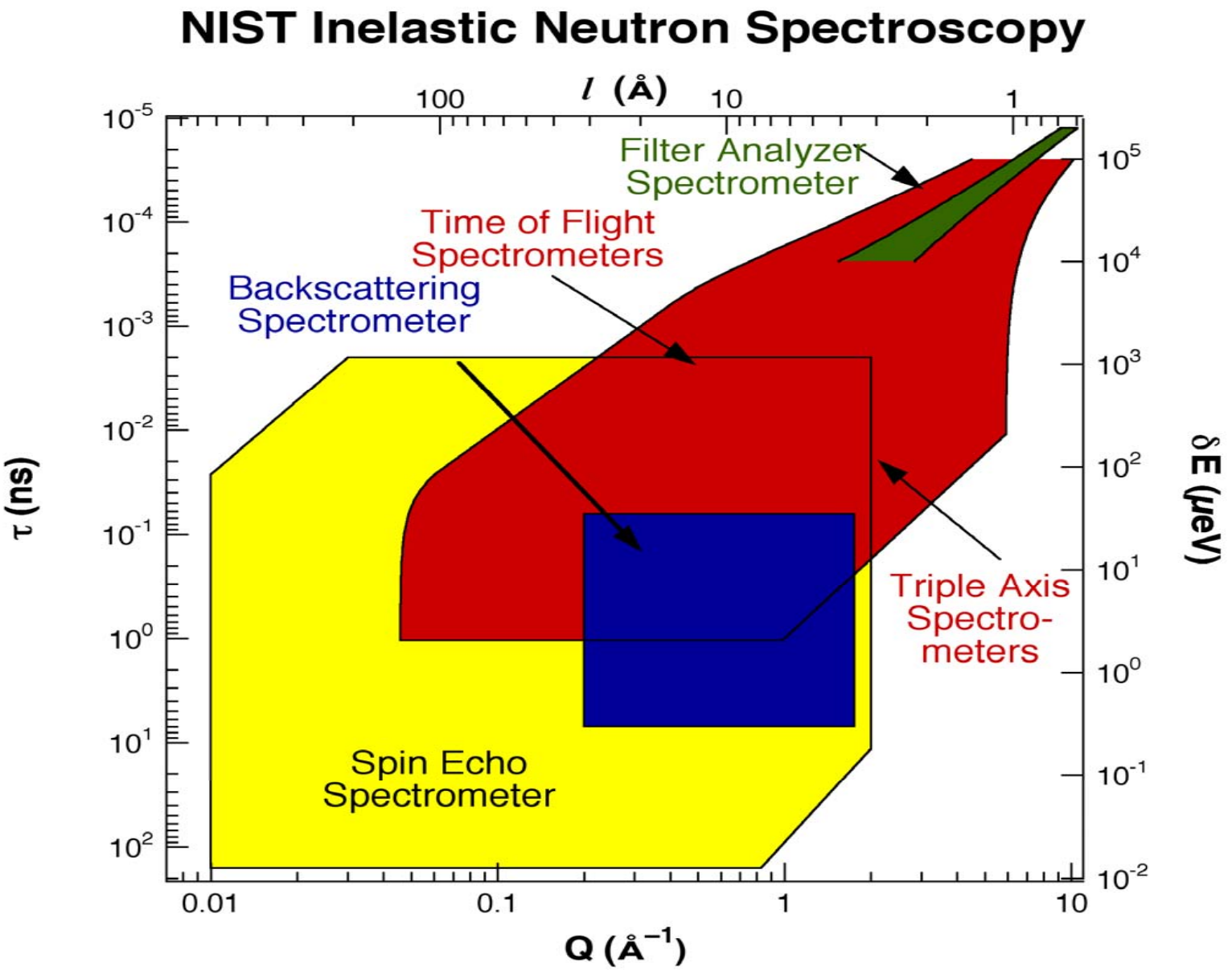

NCNR Expansion—2nd Guide Hall

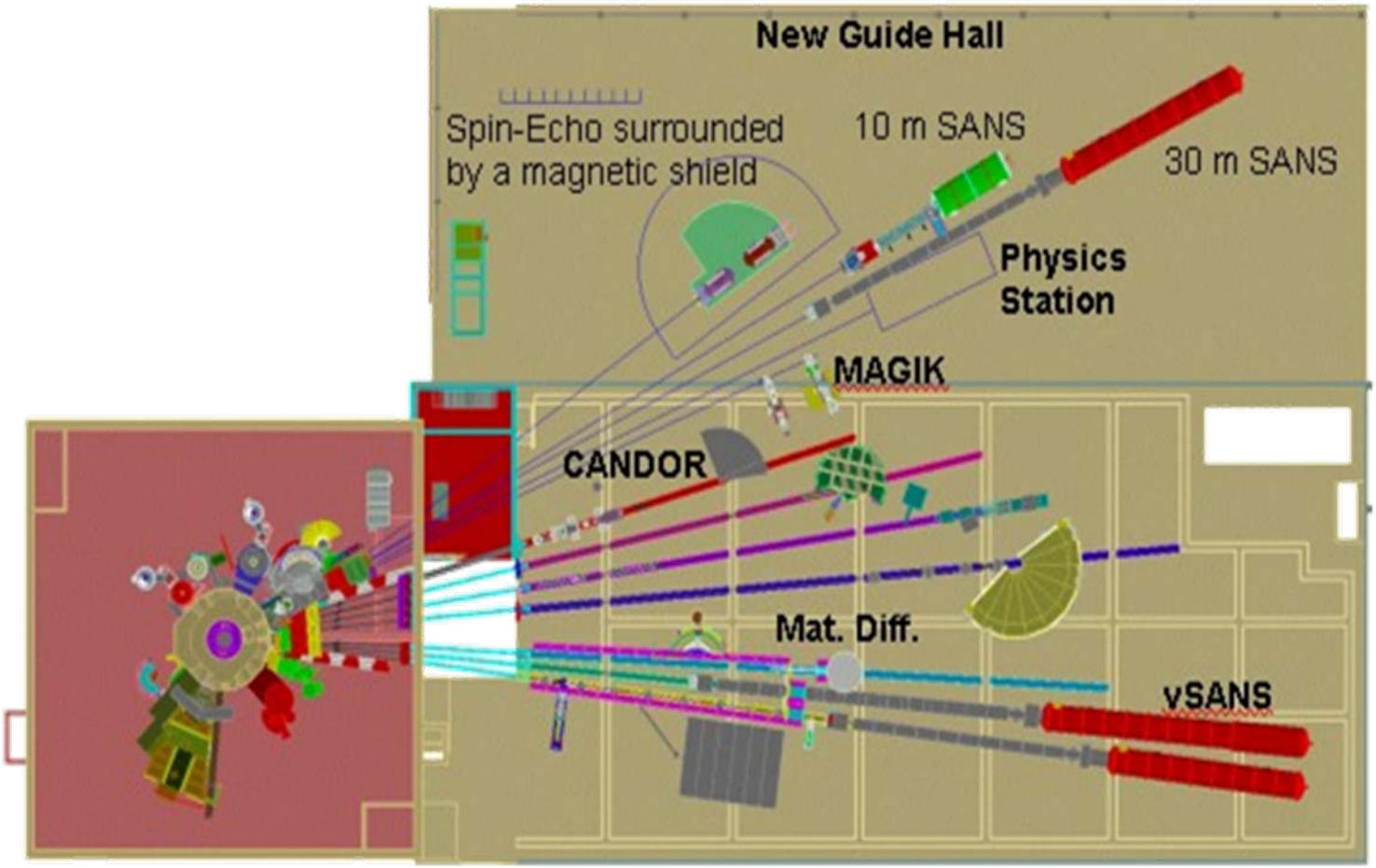

http://www.ncnr.nist.gov

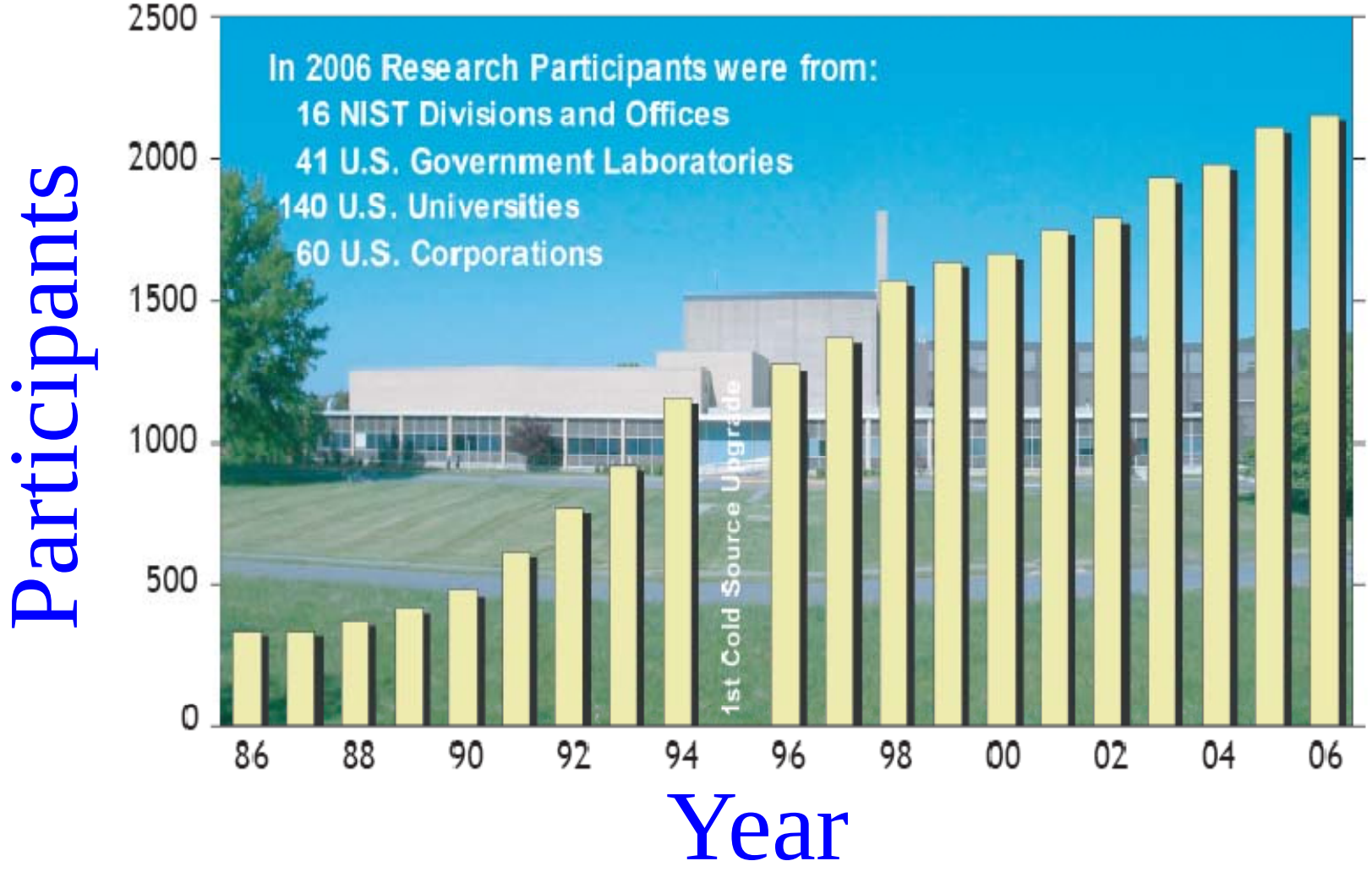

http://www.ncnr.nist.gov

Systems under Investigation with Neutron Scattering

- CMR systems, Multiferroics (La-$CaMnO_3$, $HoMnO_3$)
- Magnetic Superconductors (e.g. RNi_2B_2C, $RuSr_2GdCu_2O_8$)
- Heavy Fermion Materials ($CeRhIn_5$, $PrOs_4Sb_{12}$, …)
- Non-Fermi Liquids ($UCu_{5-x}Pd_x$, $Sc_{1-x}U_xPd_3$)
- Magnetic Order and Fluctuations in Cuprates
- Magnetic Order, Spin Fluctuations, and Crystal Structure in iron-based superconductors
- Frustrated Magnets (Spin Ice, Magnetic Monopoles, …)

– http://www/ncnr.nist.gov/staff/jeff

$La_{1-x}Ca_xMnO_3$

Phase Diagram

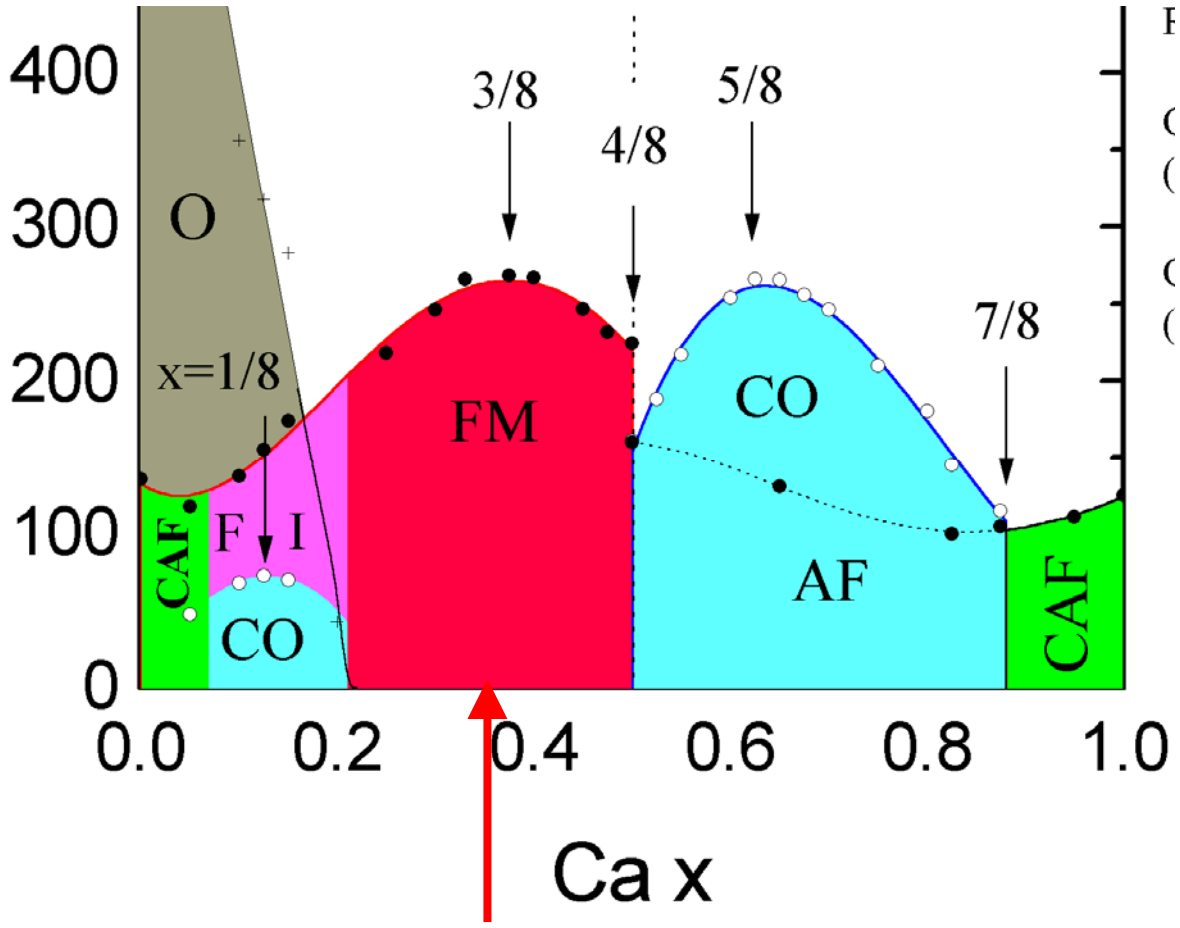

S-W. Cheong and C. H. Chen
Colossal Magnetoresistance, Charge Ordering, and Related Properties of Manganese Oxides (World Scientific, 1998), p. 241 (Ed. by Raveau and Rao)

Magnetoresistance

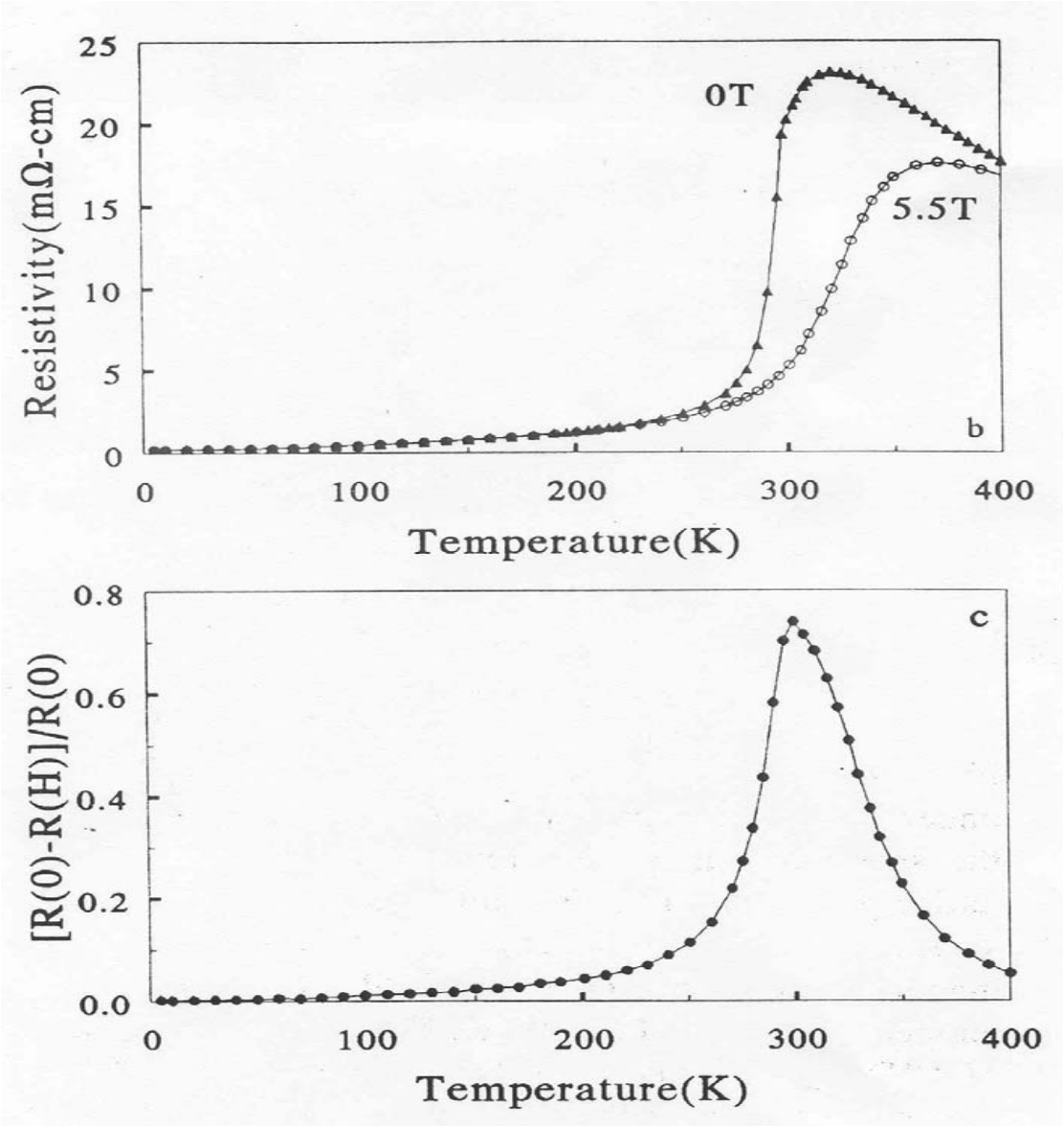

Excitations

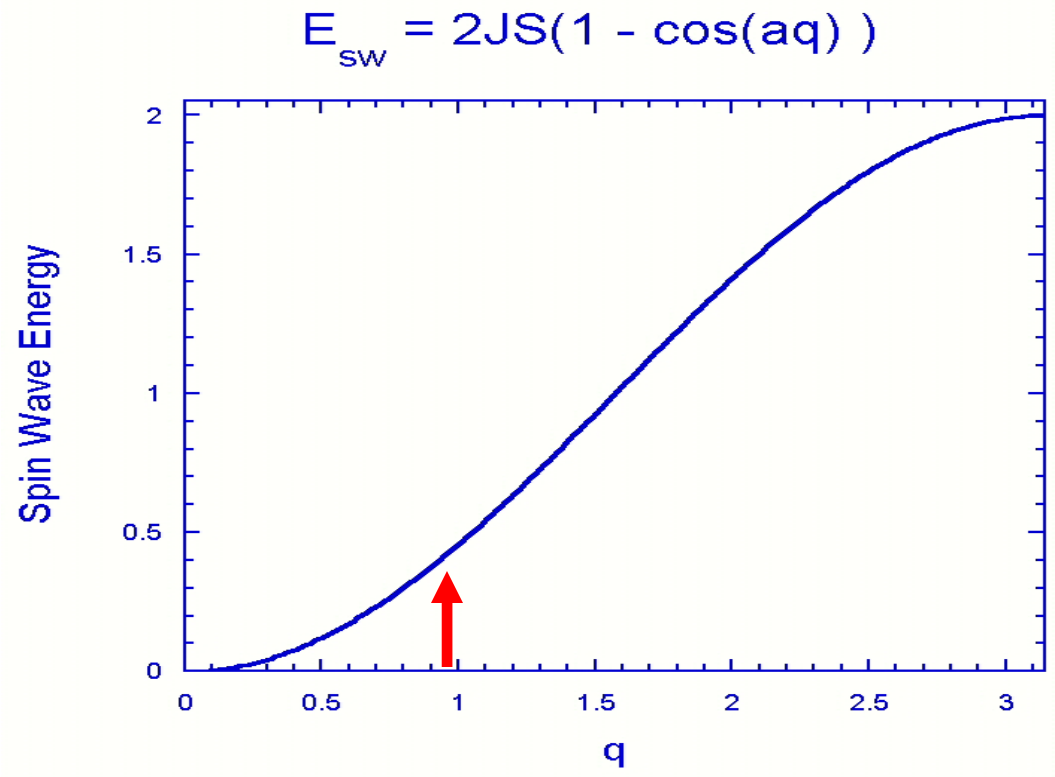

$$E_{sw} = 2JS(1 - \cos(aq)) \approx \Delta + D(T)q^2$$

$$D(T) \sim M(T)$$

$$\Gamma \sim T^2 q^4$$

Spin Dynamics

$$E_{SW} = D(T)\, Q^2$$

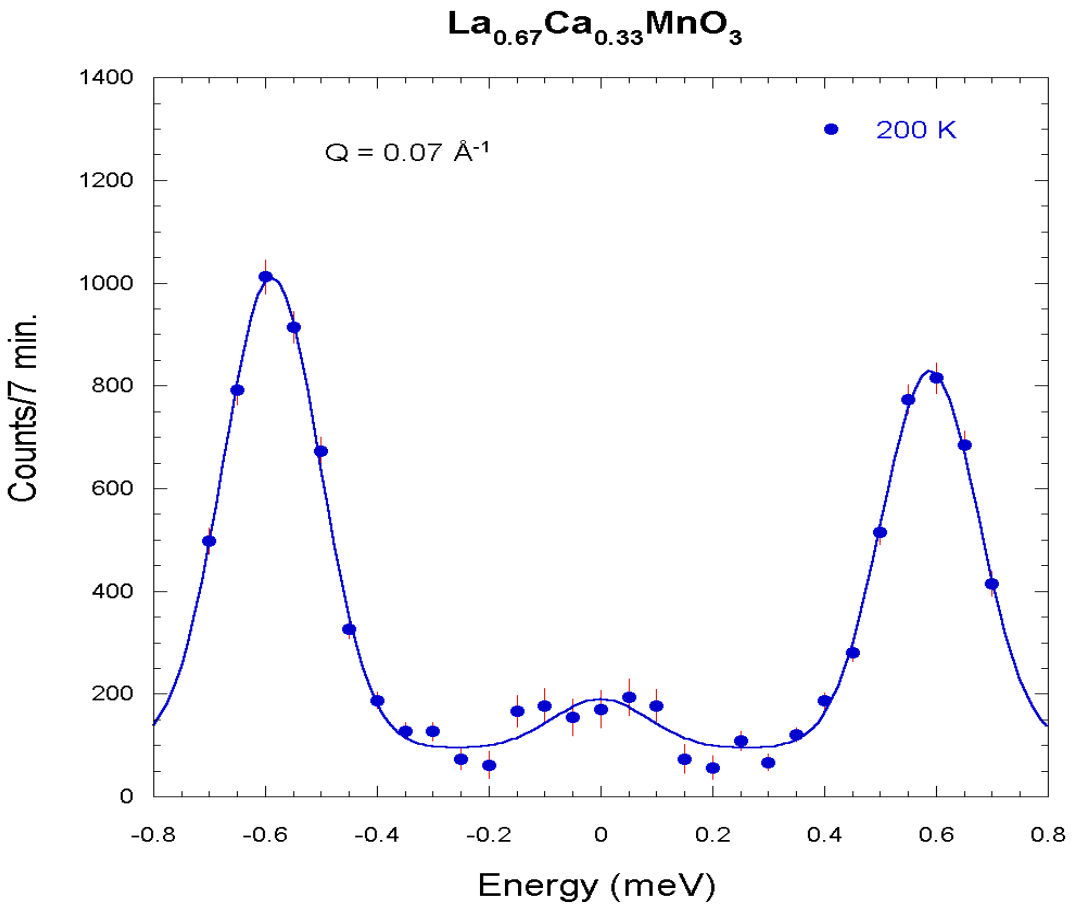

$(La_{085}Sr_{0.15})MnO_3$

Colossal Magnetoresistive Oxide

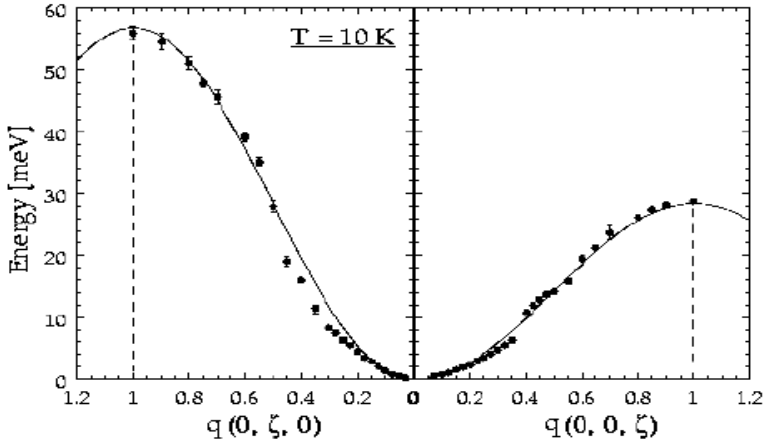

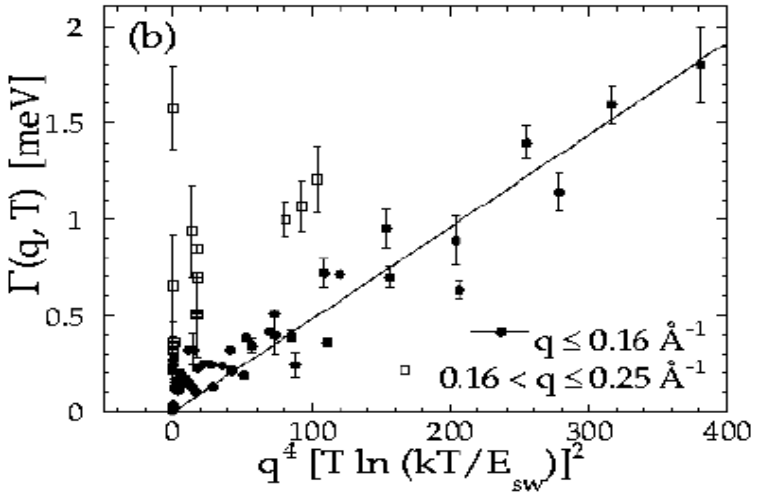

Spin Wave Excitations

$La_{0.8}Ba_{0.2}MnO_3$ *D(T)*

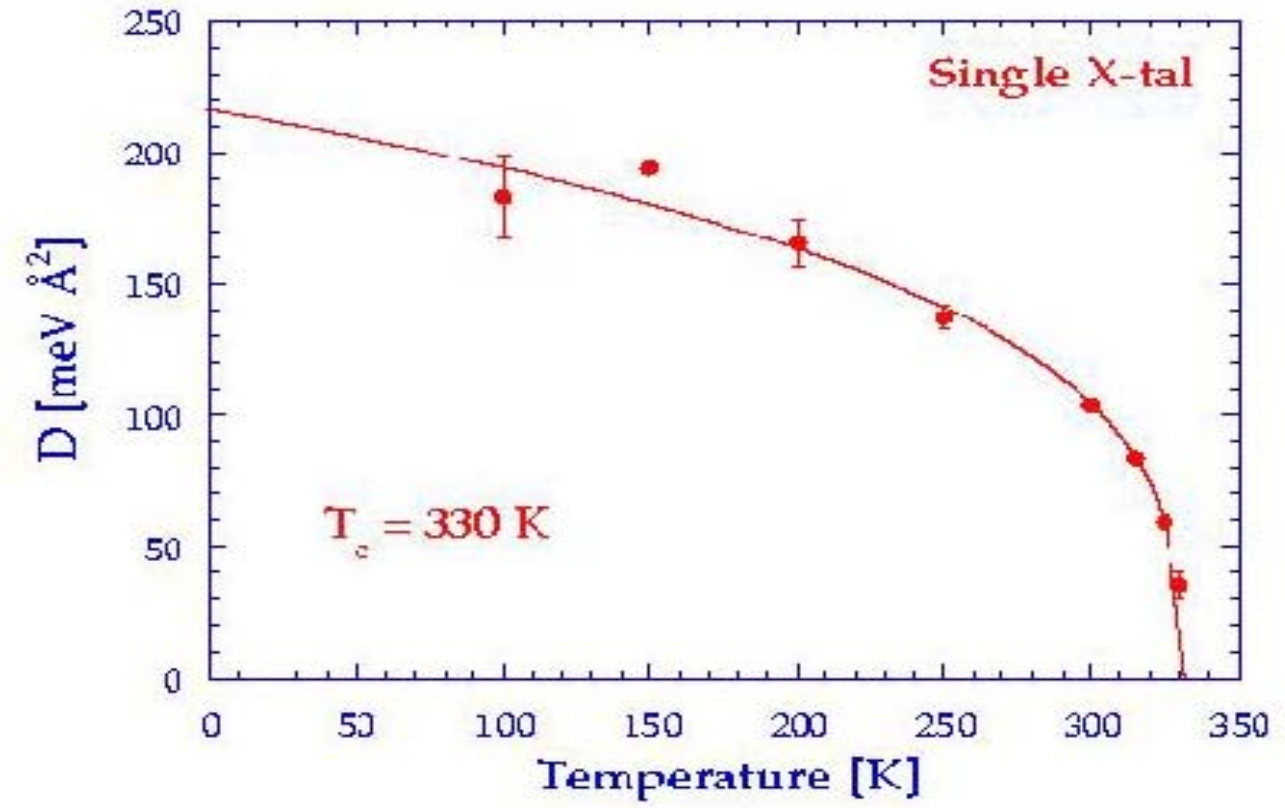

$E_{SW} = D(T)\ Q^2$

$(La_{0.7}Sr_{0.3})MnO_3$

Colossal Magnetoresistive Oxide

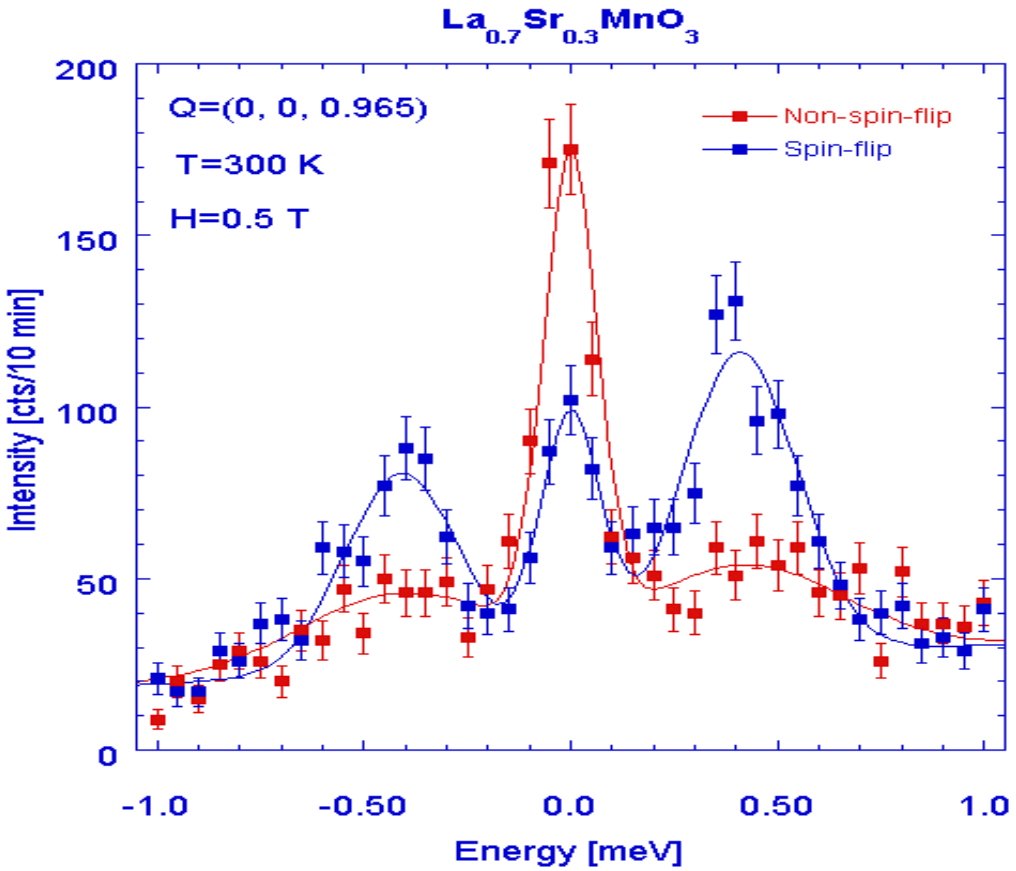

Spin Wave Excitations

And there is coupling to the Lattice

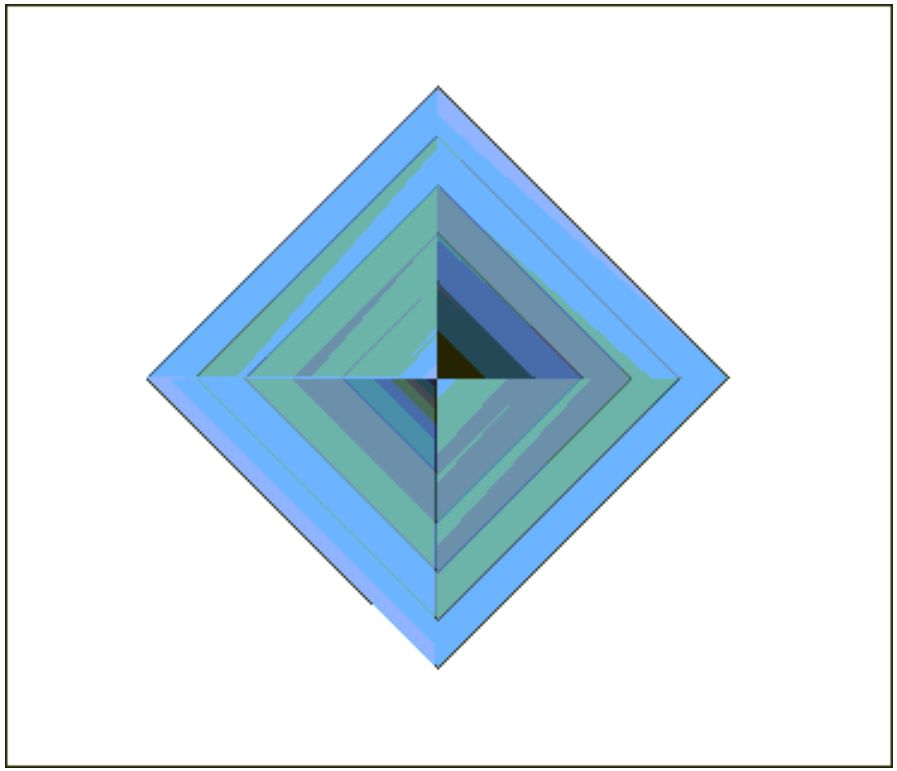

Nanoscale Correlations in CMR Manganites

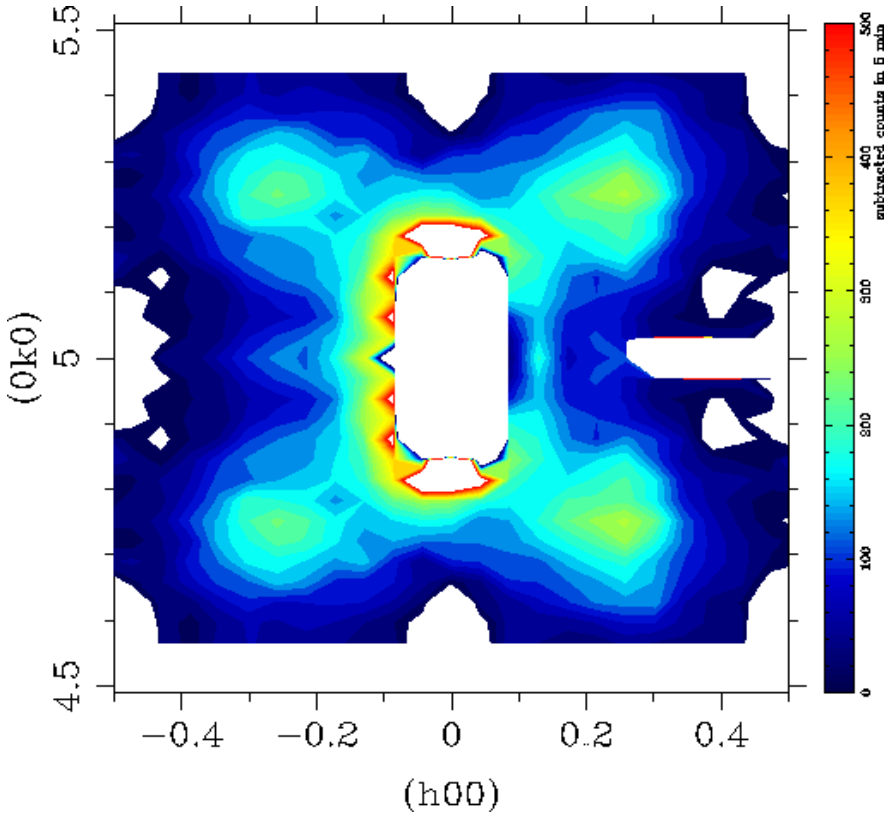

CE-type (1/4,1/4,0) peaks

Polaron Peaks

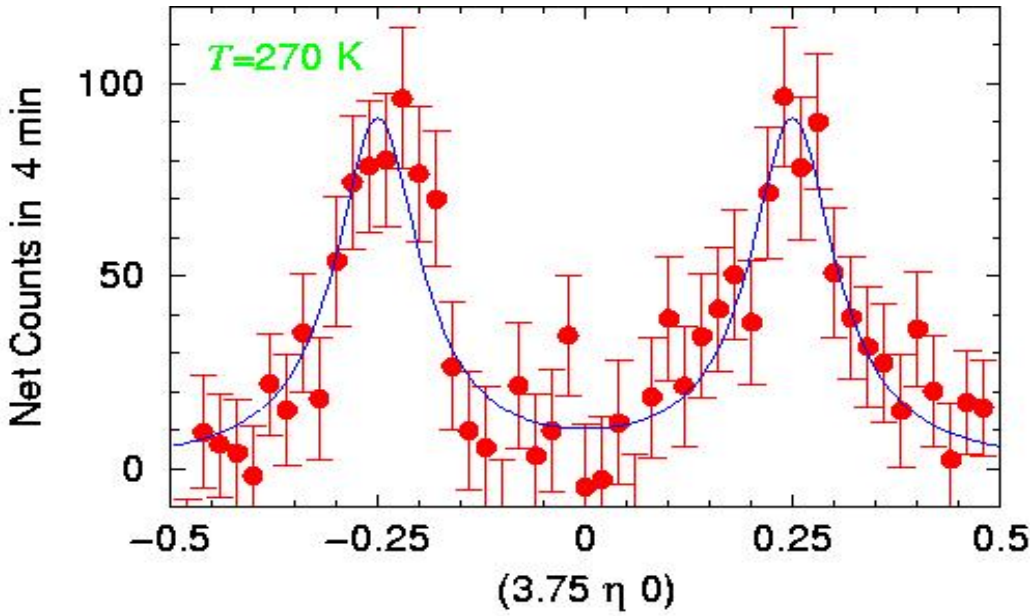

C. P. Adams, J. W. Lynn, Y. M. Mukovskii, A. A. Arsenov, and D. A. Shulyatev, Phys. Rev. Lett. **85**, 3954 (2000) .

T dependence

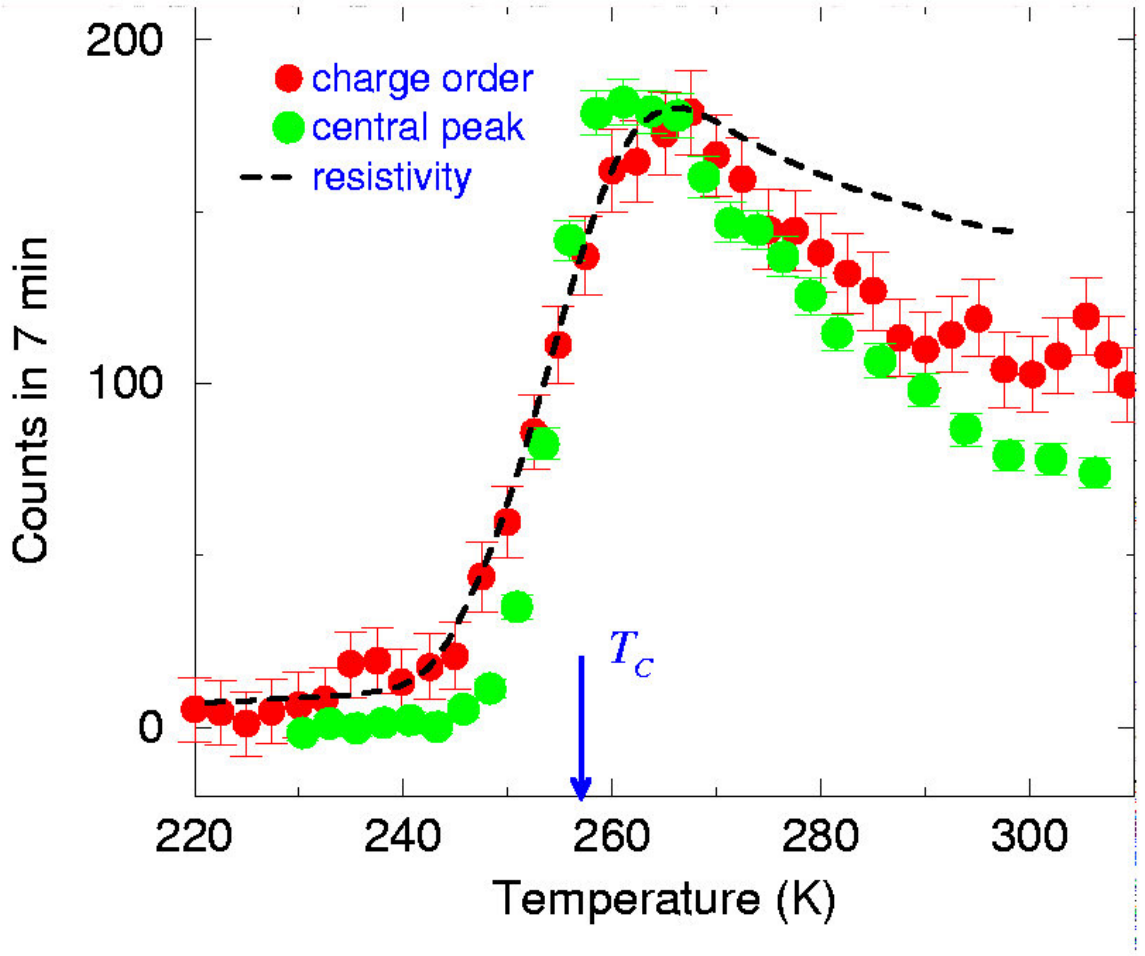

$La_{0.7}Ca_{0.3}MnO_3$ Field Dependence

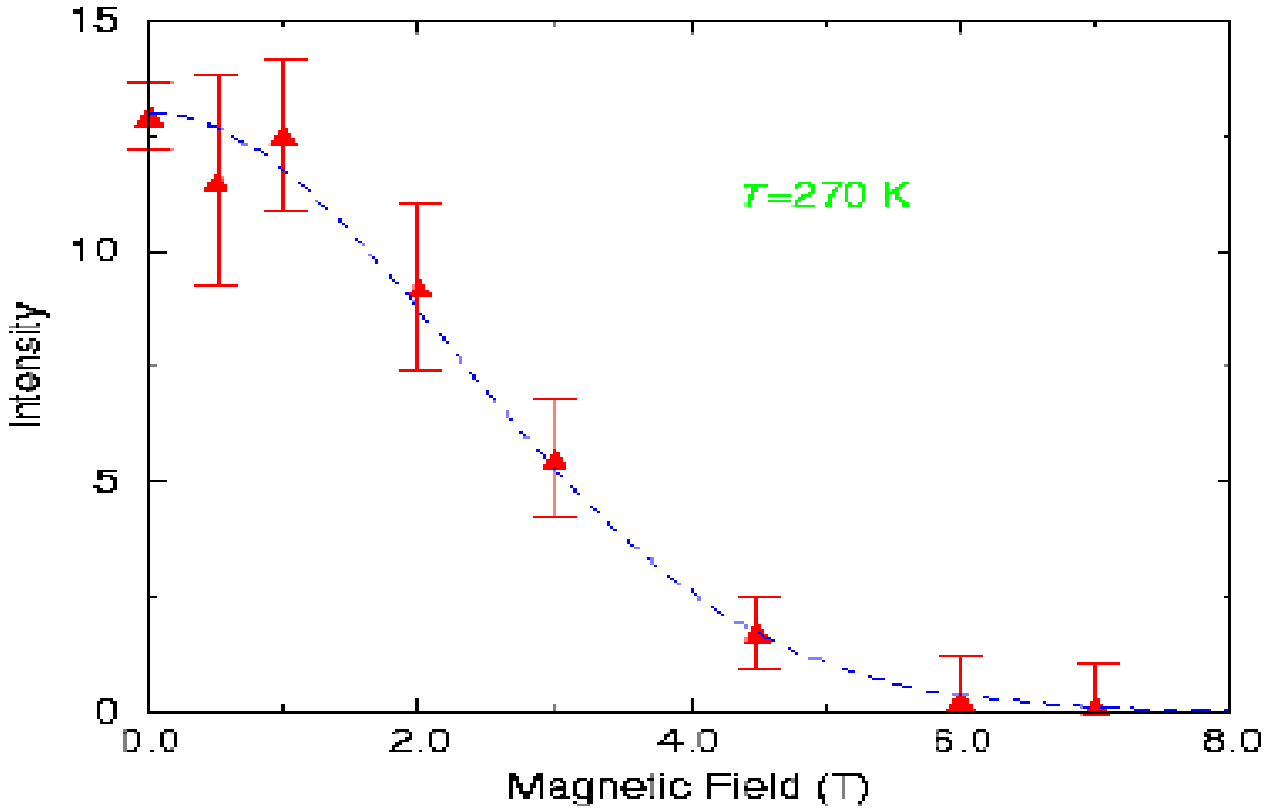

J. W. Lynn, C. P. Adams, Y. M. Mukovskii, A. A. Arsenov, and D. A. Shulyatev, J. Appl. Phys. 89, 6846 (2001).

Dynamic Polaron Correlations in the colossal magnetoresistive $La_{0.7}Ca_{0.3}MnO_3$ system

(¼, ¼,0) peaks

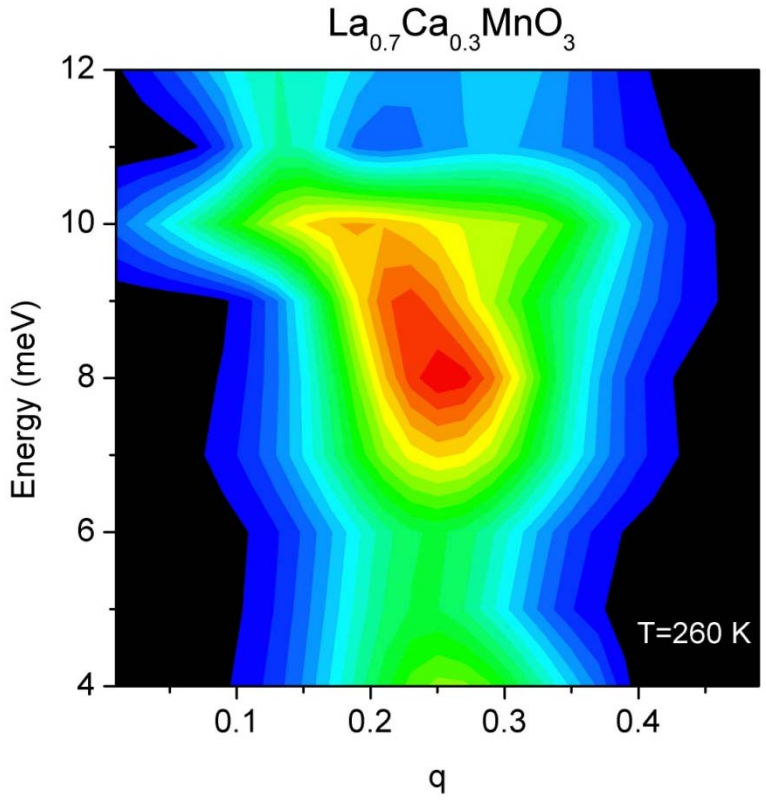

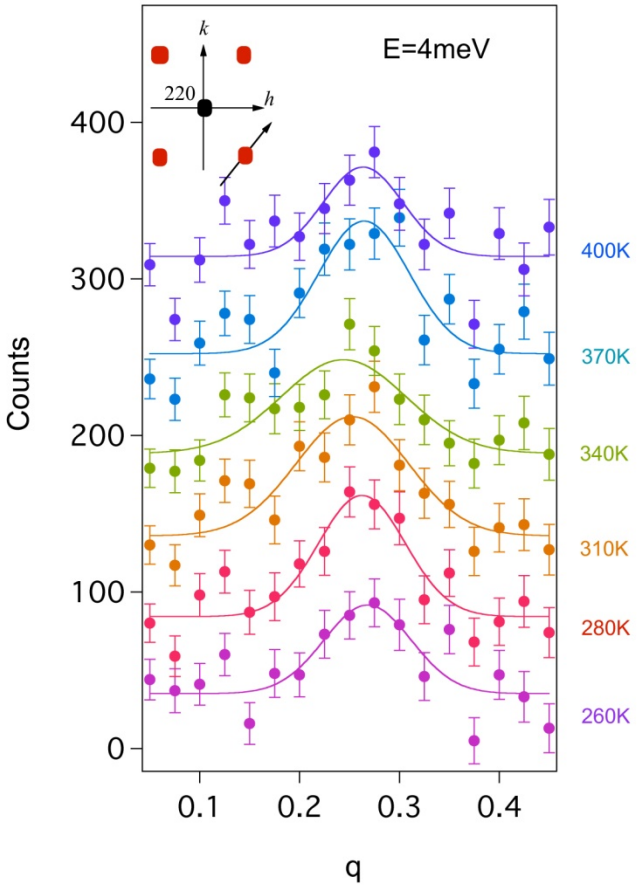

Phys. Rev. B **76**, 014437 (2007)

La-$CaMnO_3$ Polarons

PSD mode

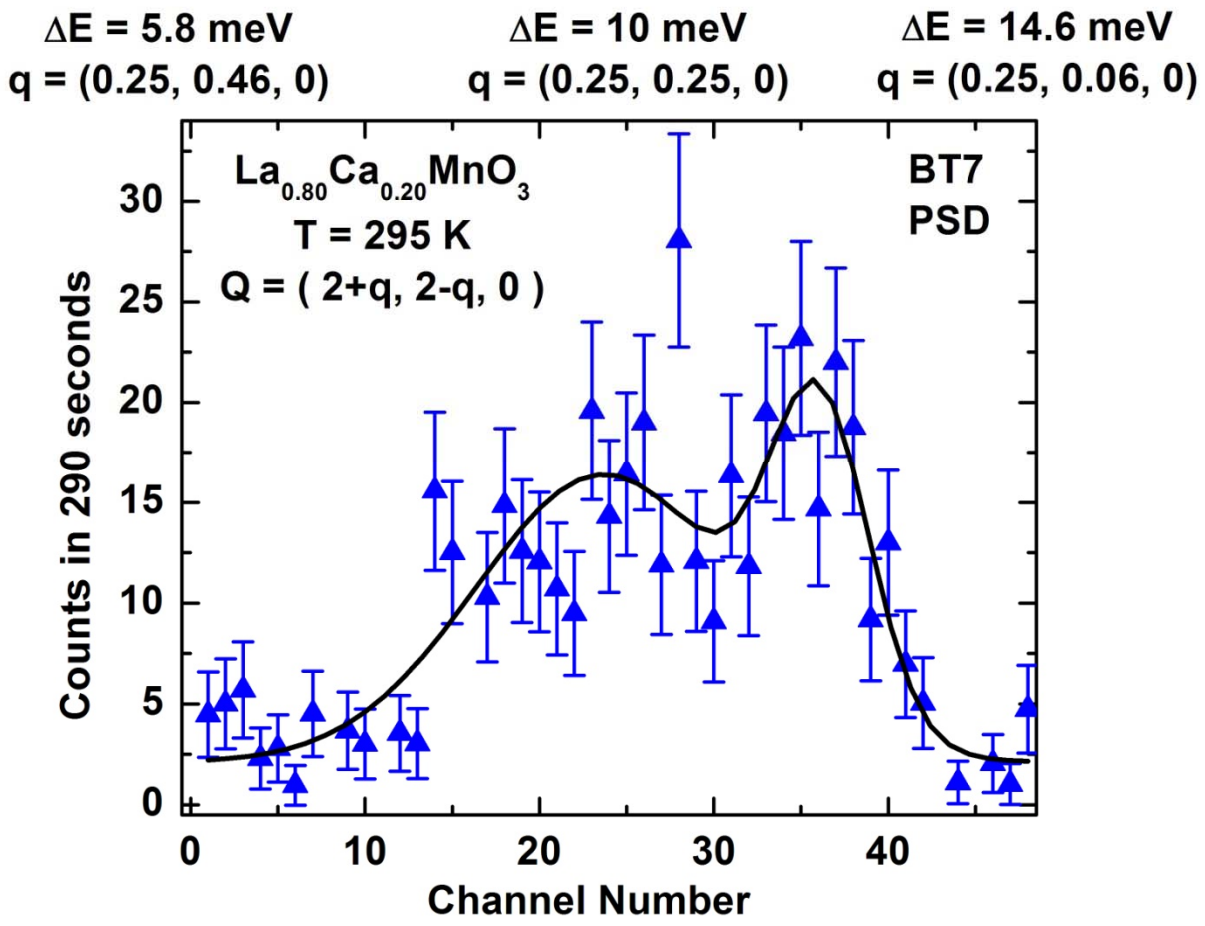

Phonons in Gold

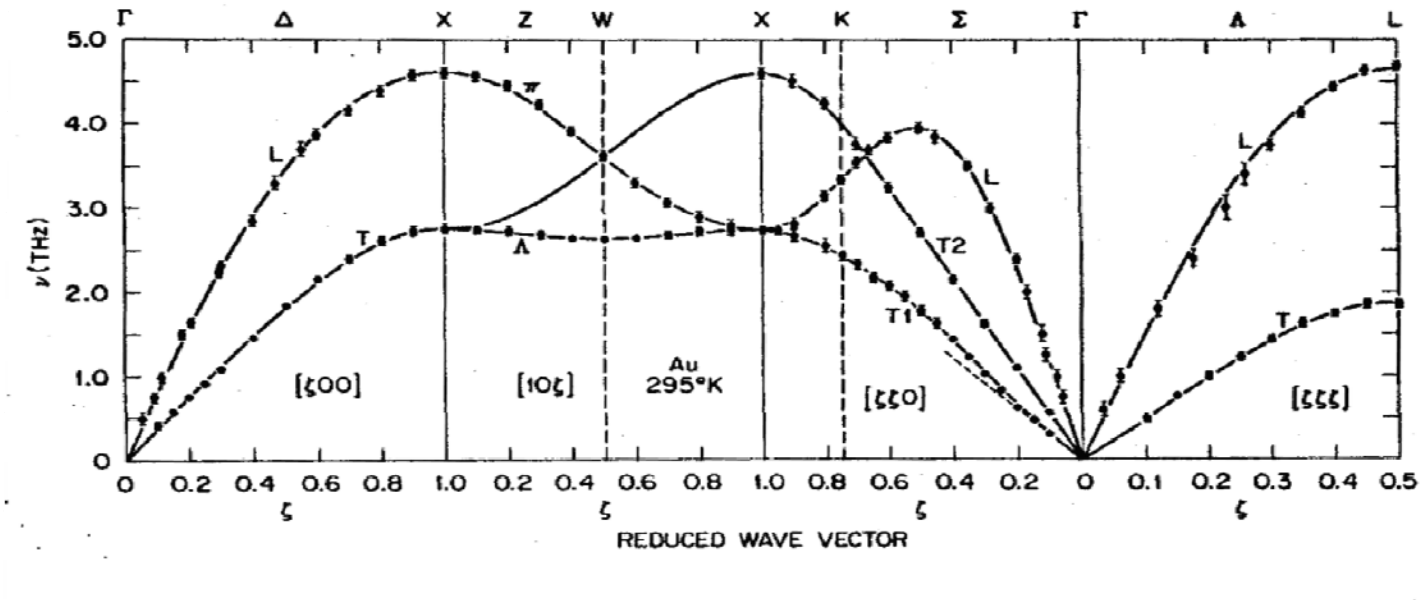

Three phonon modes

Phonon Density of States in Noble Metals

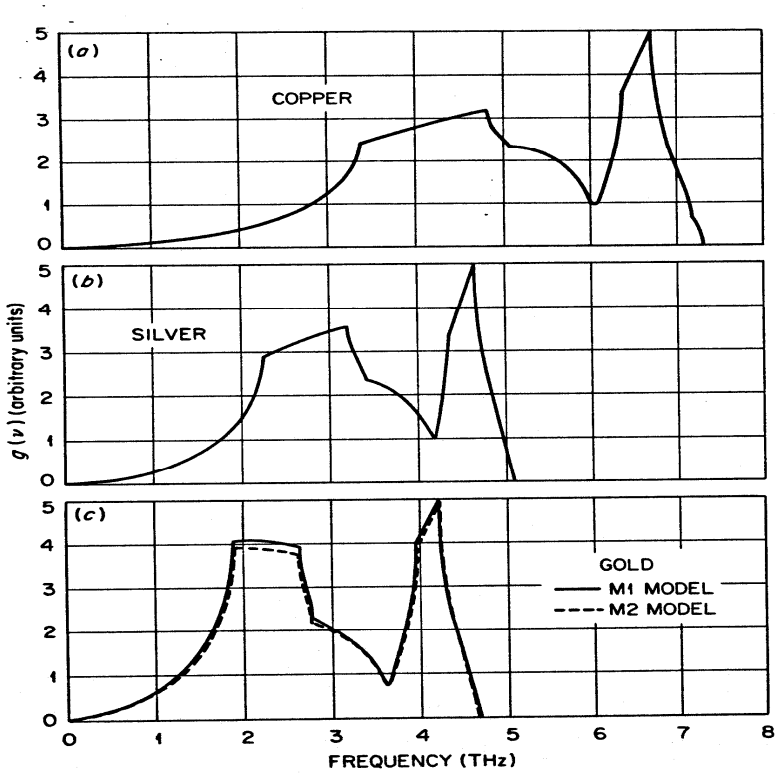

AgBr Phonons

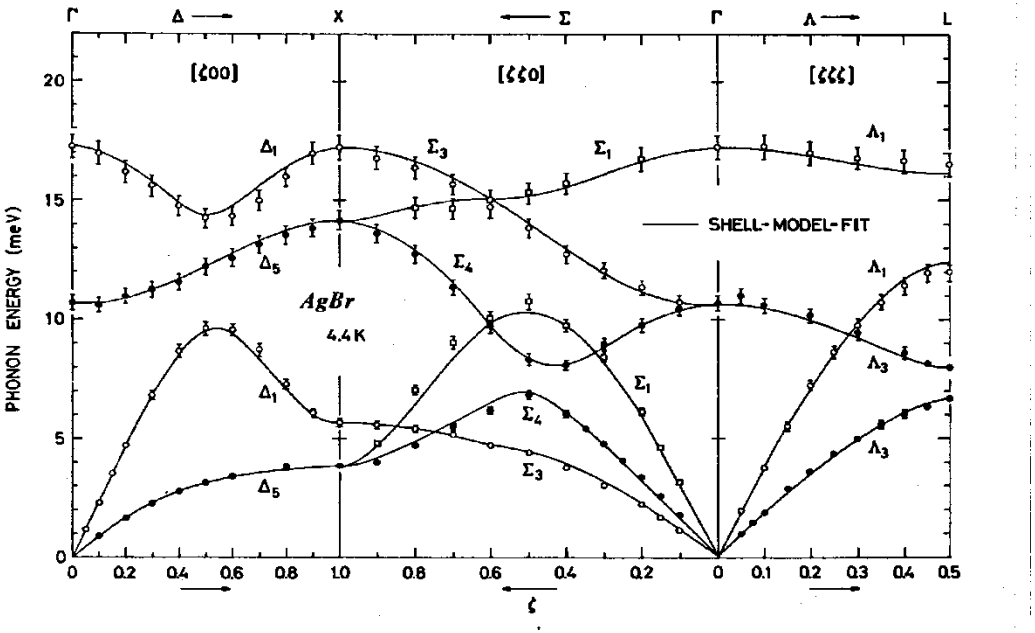

Phonon Density of States in MgB_2
T_C=39K (FANS)

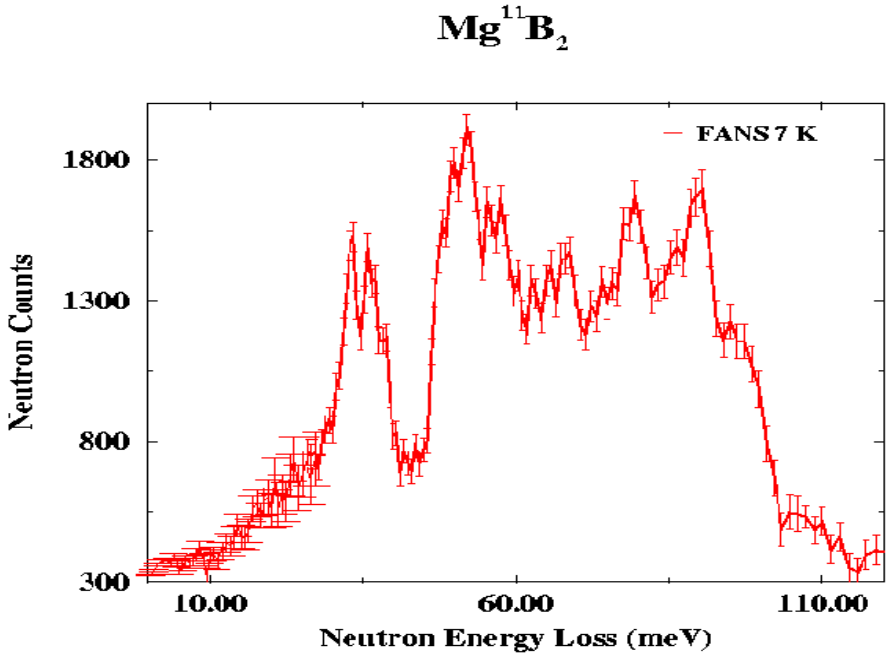

Spin Echo Data

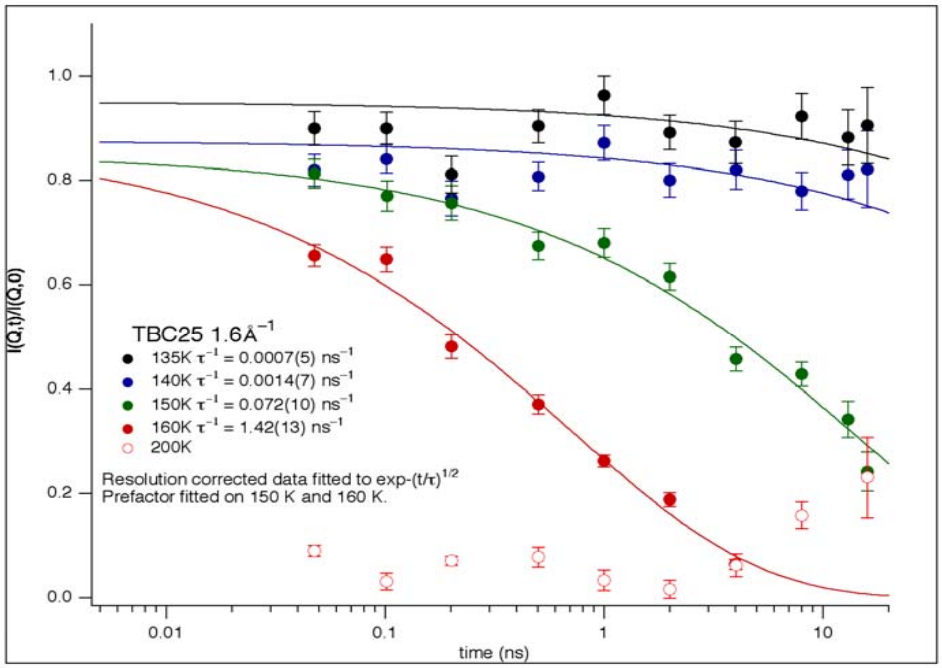

Intermediate scattering function of Toluene with 25% Benzyl Chloride at the structure factor peak above the glass temperature. The data are fitted with a stretched exponential using the usual exponent of 1/2.

1. The correlation time increases with decreasing temperature, as one might expect, and also agrees with results from NMR.
2. The data do not extrapolate to 1 at t=0 because there is another faster relaxation process.

Quantum Rotational Tunneling in Toluene: A Measurement using HFBS

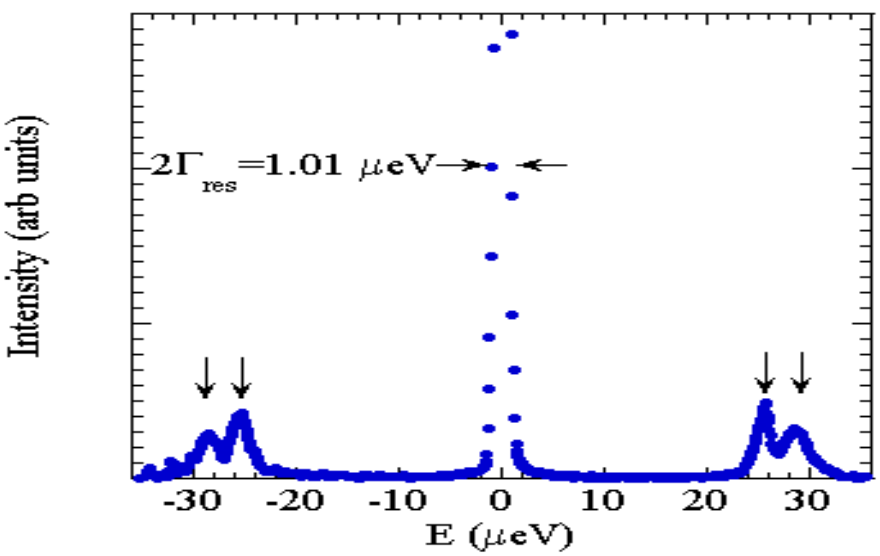

- Motion of methyl groups (CH_3) in toluene ($C_6H_5CH_3$)
- Inelastic peaks correspond to tunneling through a potential barrier: a classically forbidden motion!
- Tunneling rate ~6 GHz
- Presence of two inelastic peaks on the energy loss side and two peaks on the energy gain side indicates two inequivalent sites for molecules in the solid

Spin Dynamics

$$E_{SW} = D(T)\, Q^2$$

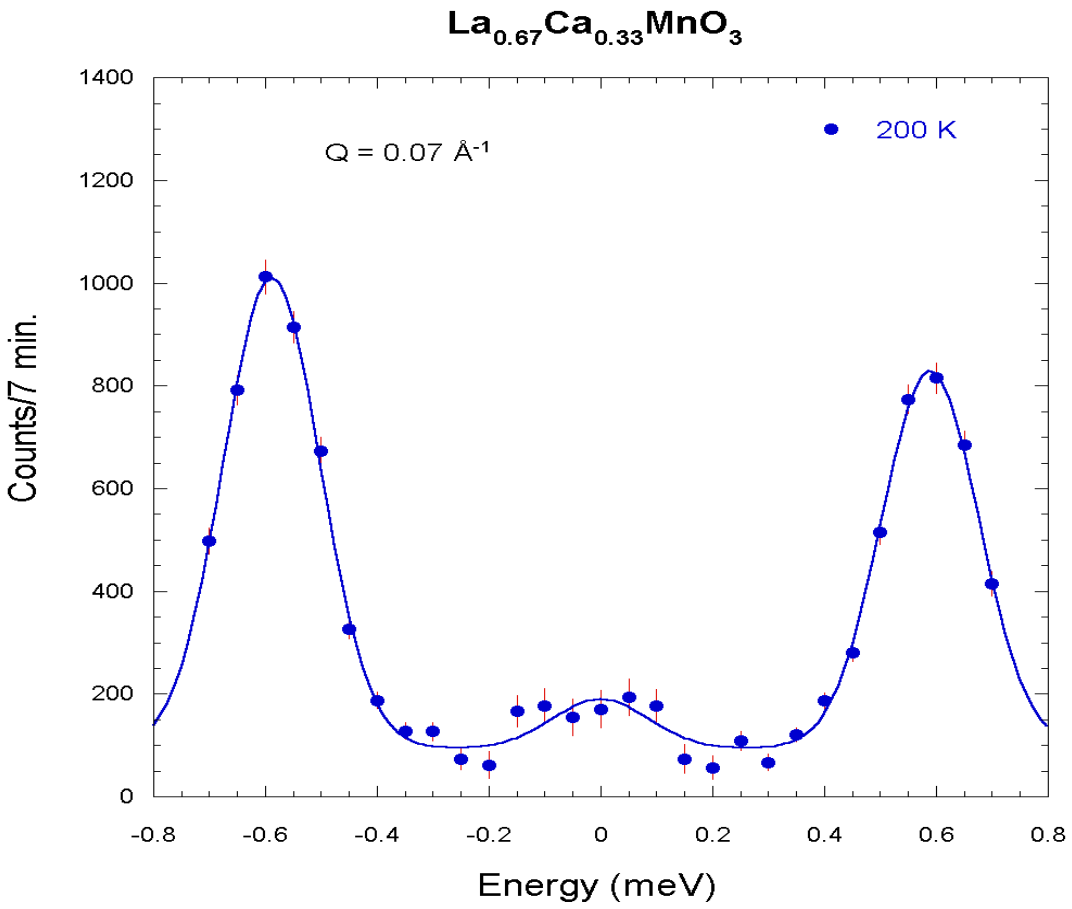

Quantum Rotational Tunneling in Toluene: A Measurement using HFBS

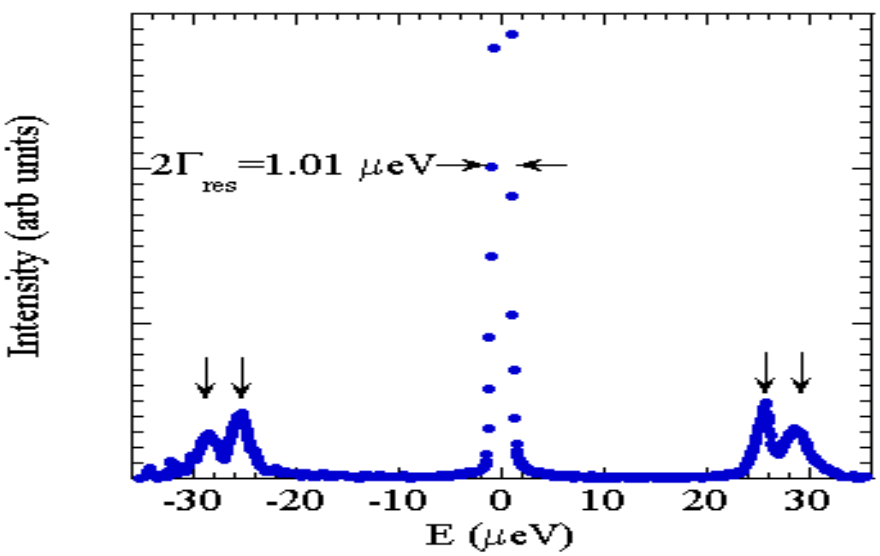

- Motion of methyl groups (CH_3) in toluene ($C_6H_5CH_3$)
- Inelastic peaks correspond to tunneling through a potential barrier: a classically forbidden motion!
- Tunneling rate ~6 GHz
- Presence of two inelastic peaks on the energy loss side and two peaks on the energy gain side indicates two inequivalent sites for molecules in the solid

Vortex Matter in Superconductor Nb (SANS)

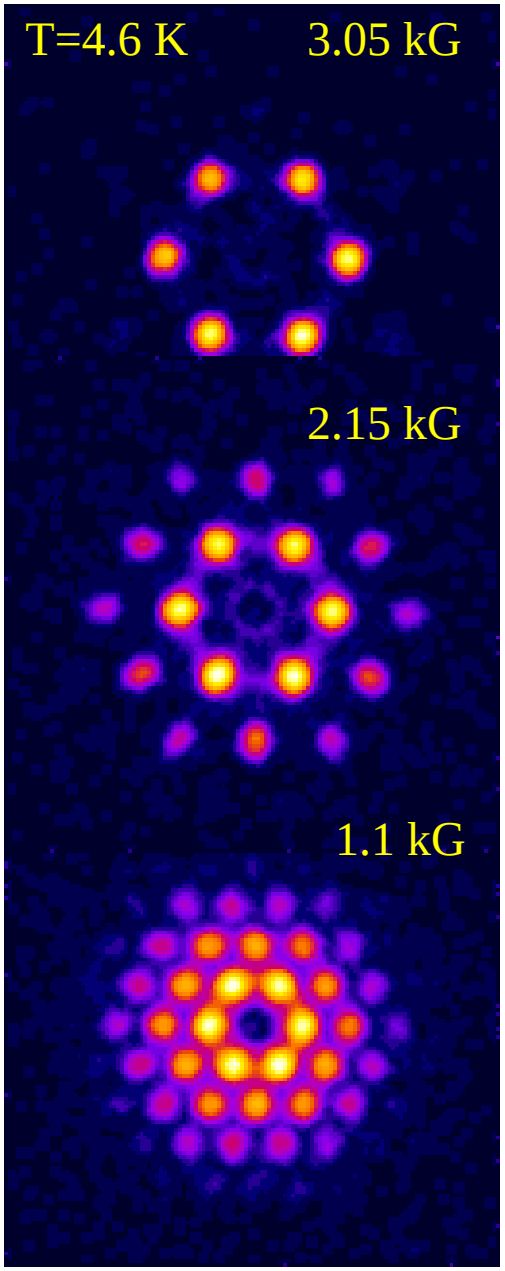

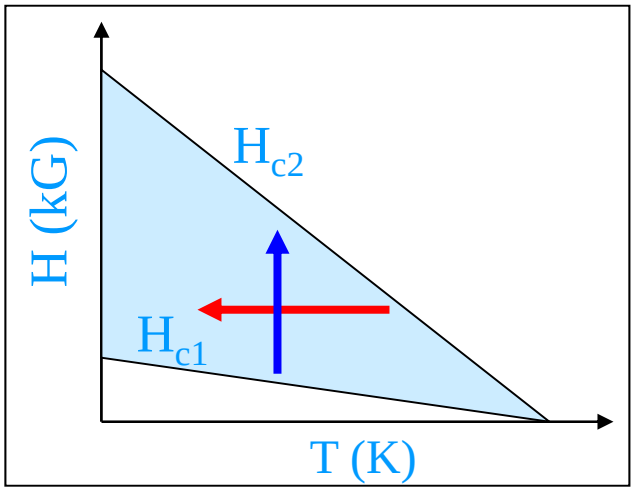

Real space depiction of vortex lattice

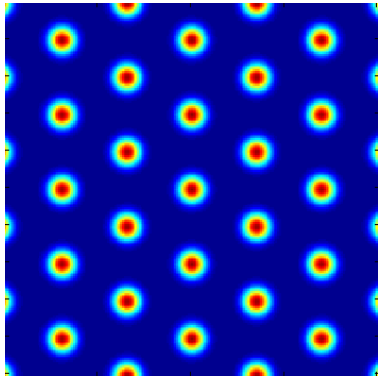

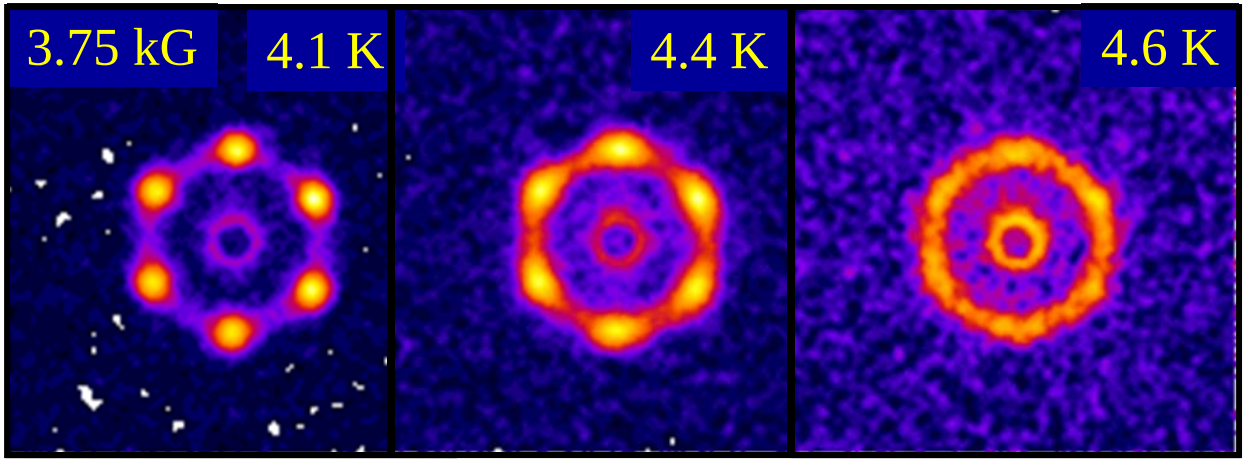

X. S. Ling, B. A. McClain and S.-R. Park (Brown University)
S.-M Choi, D. Dender and J. W. Lynn, (NCNR/NIST)
Phys. Rev. Lett. **86**, 712 (2001).

YBCO Vortex

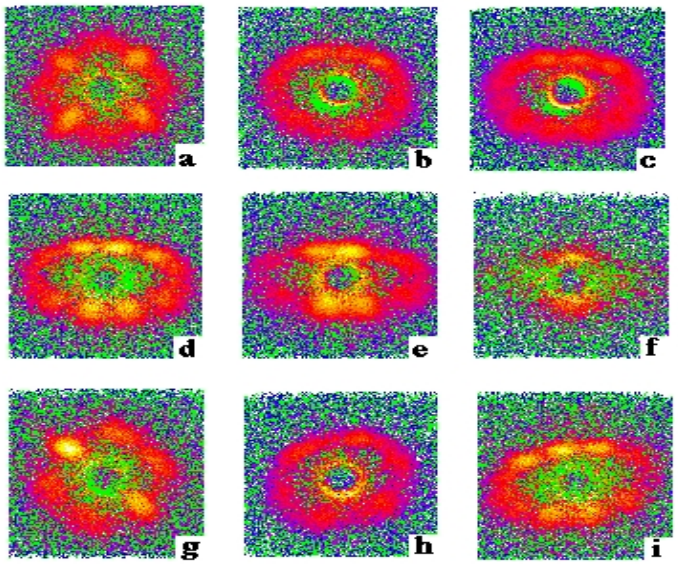

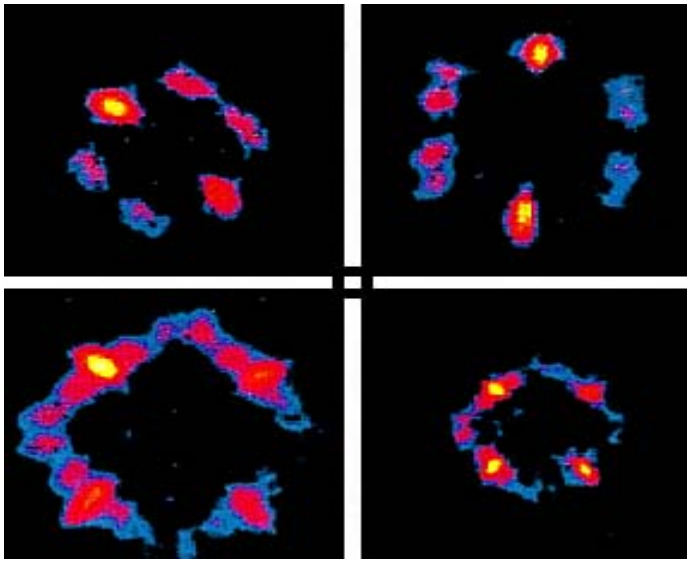

Quantum Critical Behaivor

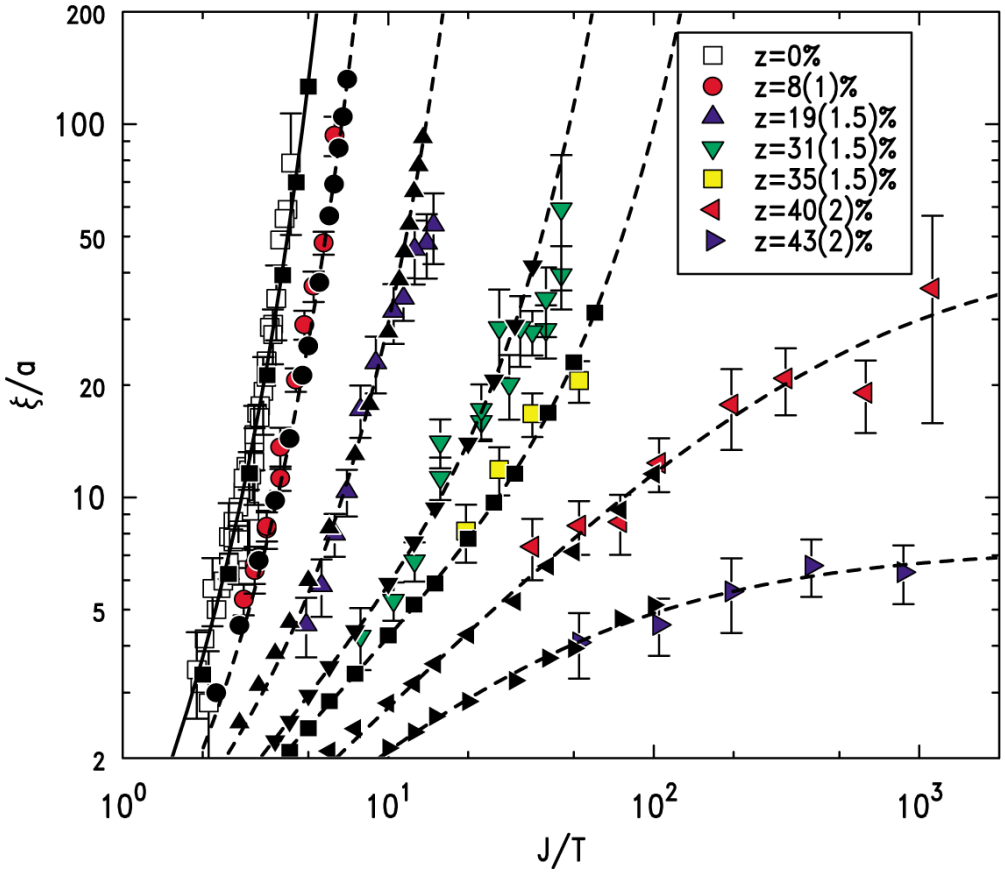

$La_2Cu_{1-x}(MgZn)_xO_4$

Quantum Impurities in the two-dimensional spin ½ Heisenberg antiferromagnet, O.P. Vajk, P.K. Mang, M. Greven, P. M. Gehring, and J.W. Lynn, Science **295**, 1691 (2002).

Magnetic Order in Cuprate Superconductors

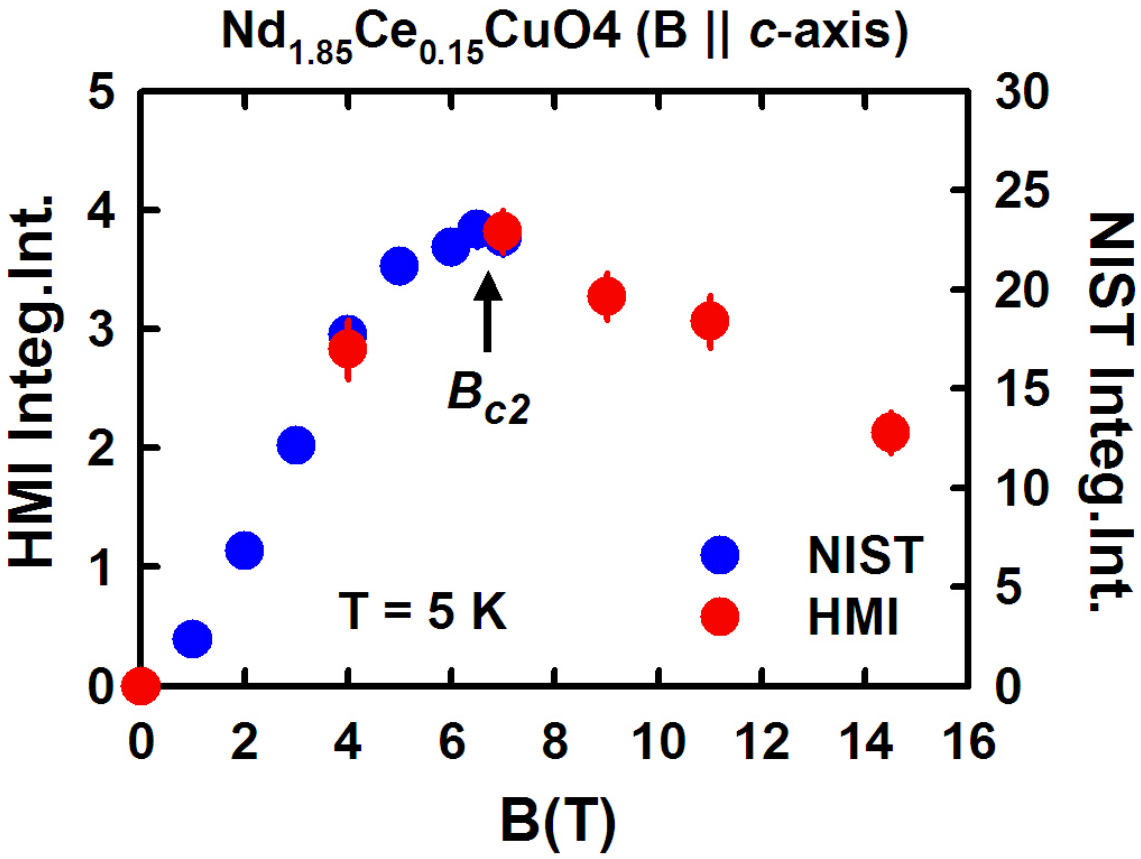

H. J. Kang, P. Dai, J. W. Lynn, M. Matsuura, J. E. Thompson, S-C Zhang, D. N. Argyriou, Y. Onose, and Y. Tokura, Nature **423**, 522 (2003).

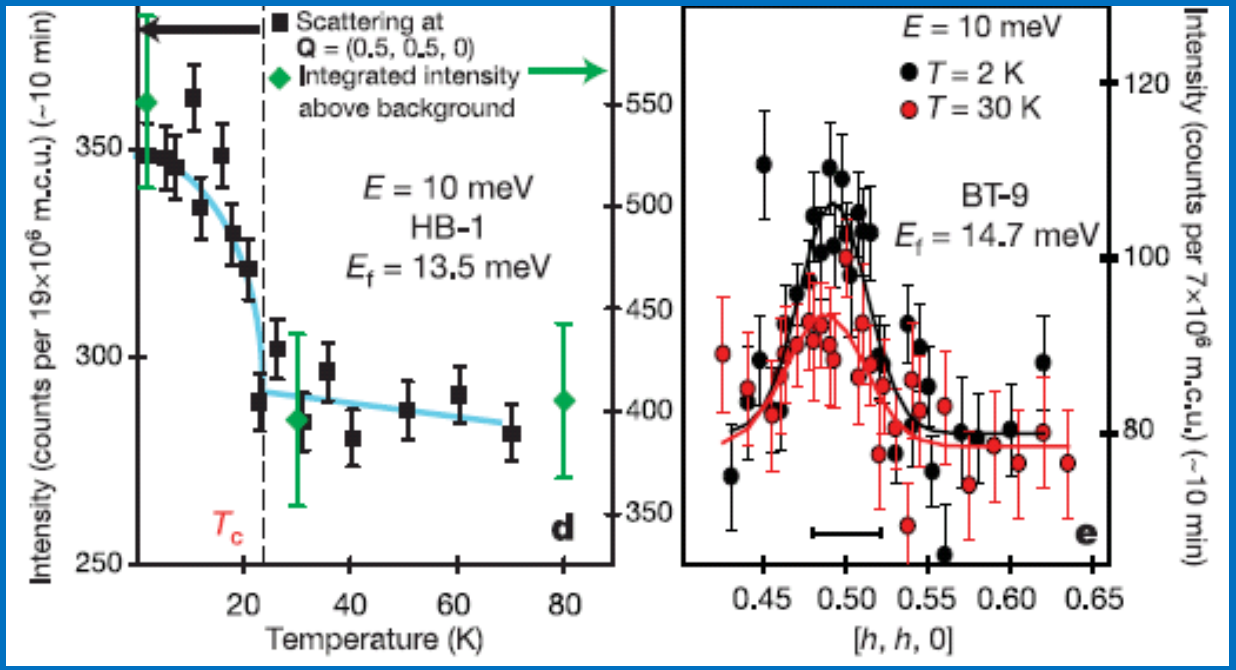

Temperature and energy dependence of the scattering around 10 meV for PLCCO (Tc = 24 K). Consistent with resonance in hole-doped materials.

S. D. Wilson, P. Dai, S. Li, S. Chi, H. Kang, & J. W. Lynn, Nature 442, 59 (2006).

Summary of neutron results

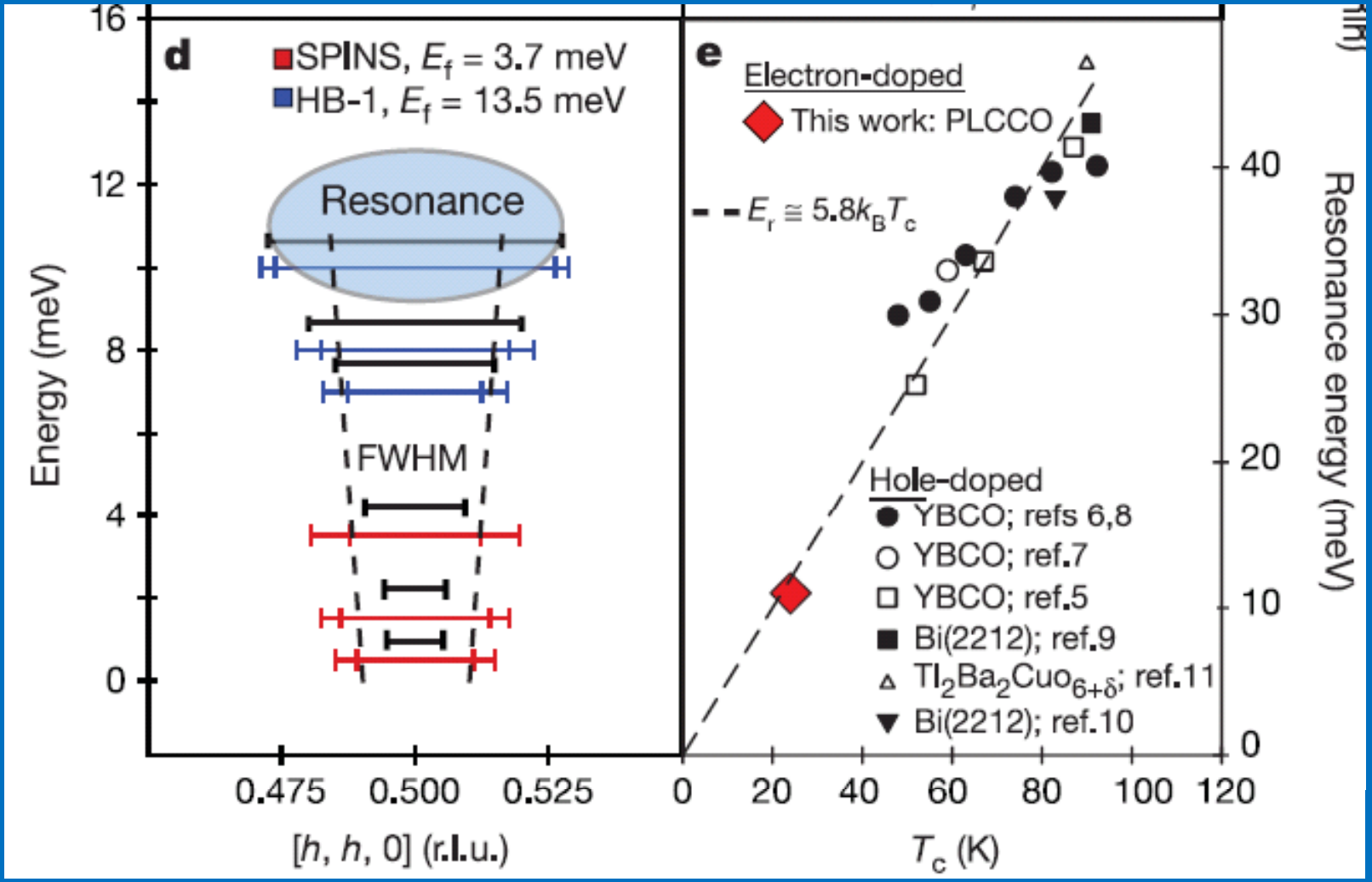

So the picture of spin excitations through superconducting-normal phase transition is:

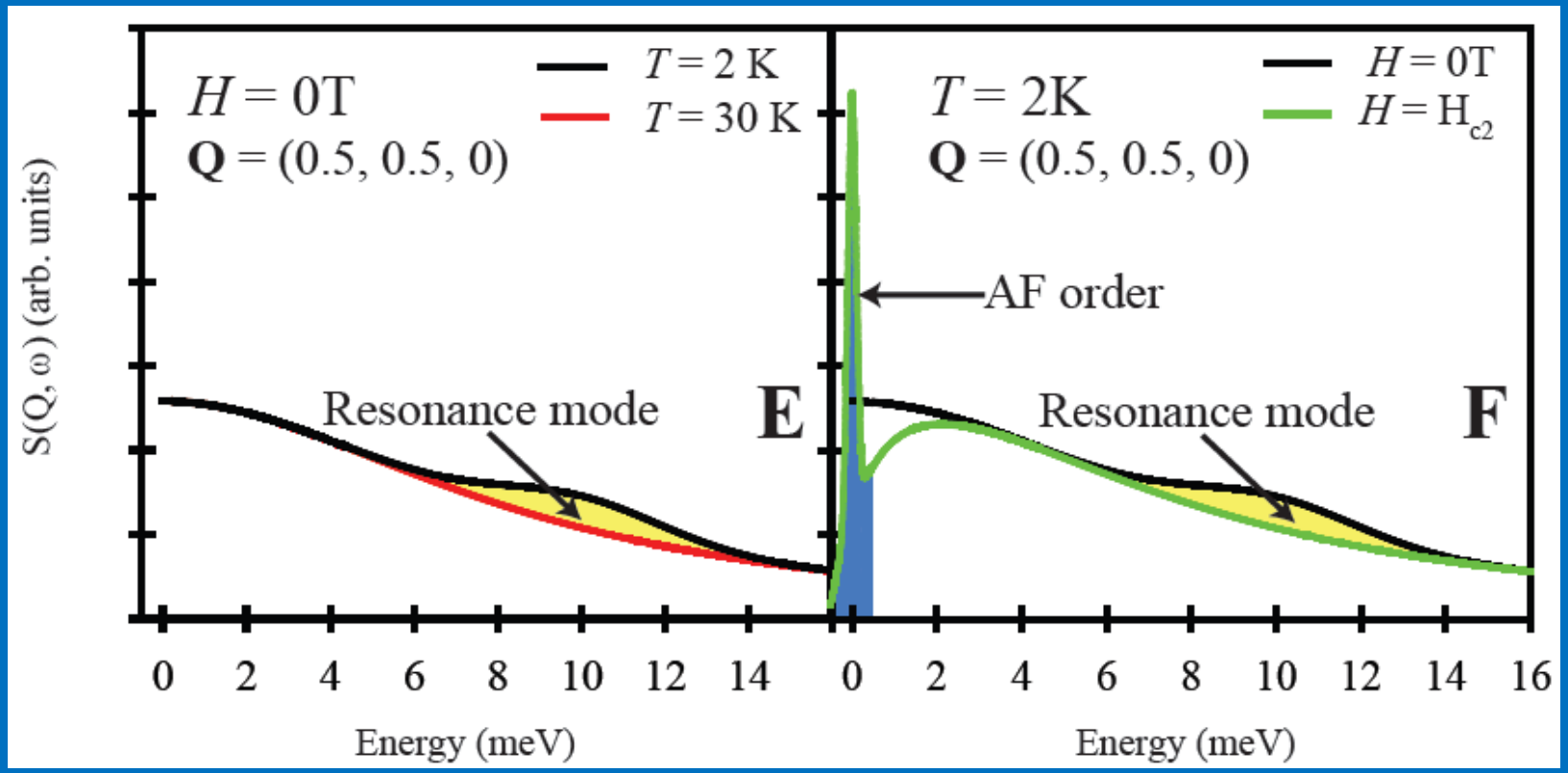

There is a direct competition between superconducting phase without AF order and the AF phase without superconductivity.

Spin wave Dispersion in Magnetostrictive Fe-Ga alloys

(With old analyzer)

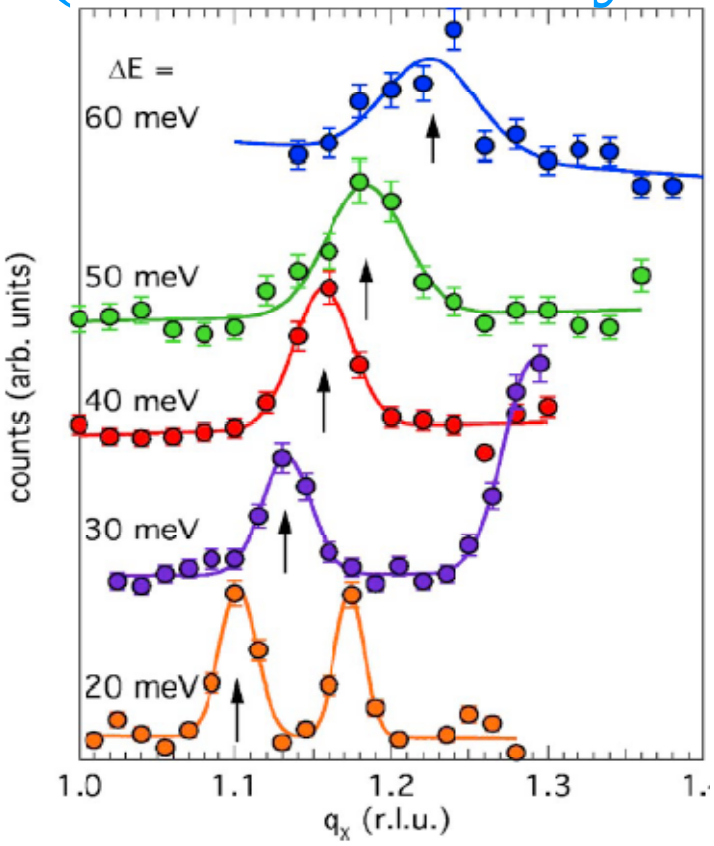

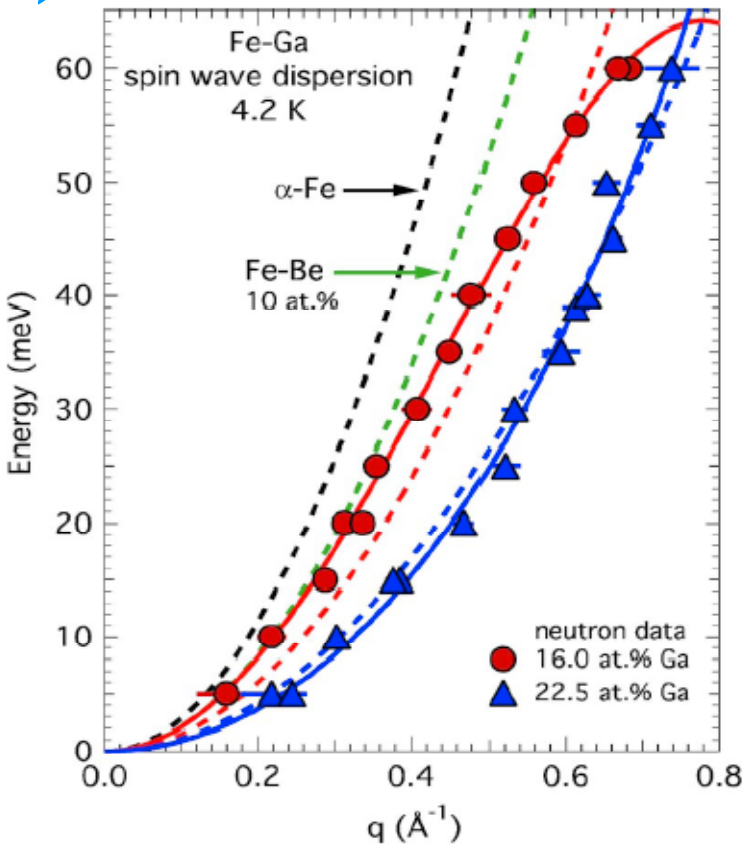

J. L. Zarestky, O. Moze, J. W. Lynn, Y. Chen, T. A. Lograsso, and D. L. Schlagel, Phys. Rev. B**75**, 052406 (2007).

Magnetic Scattering from La(O,F)FeAs

PSD
BT-7

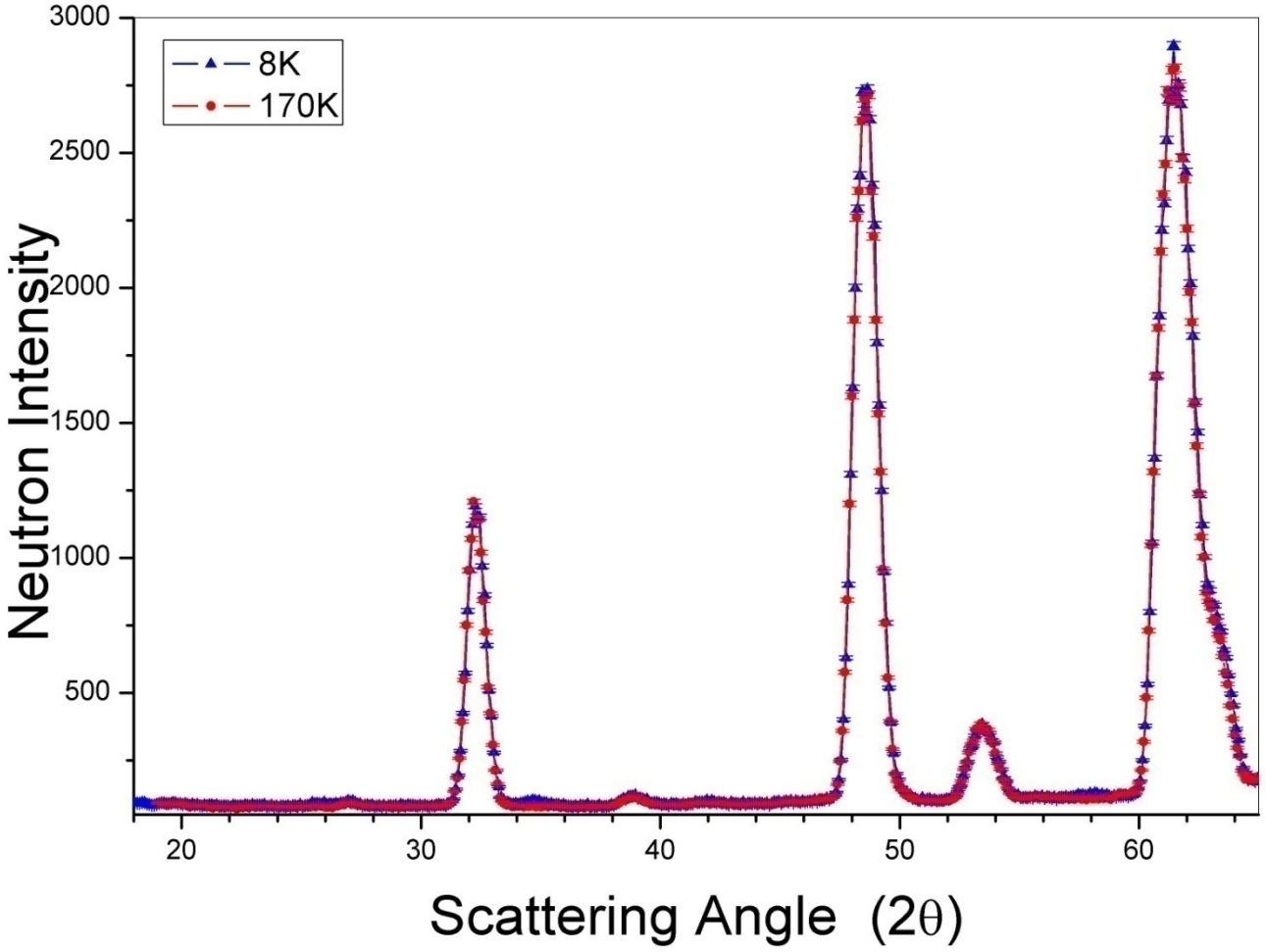

Magnetic Structure of La(O,F)FeAs

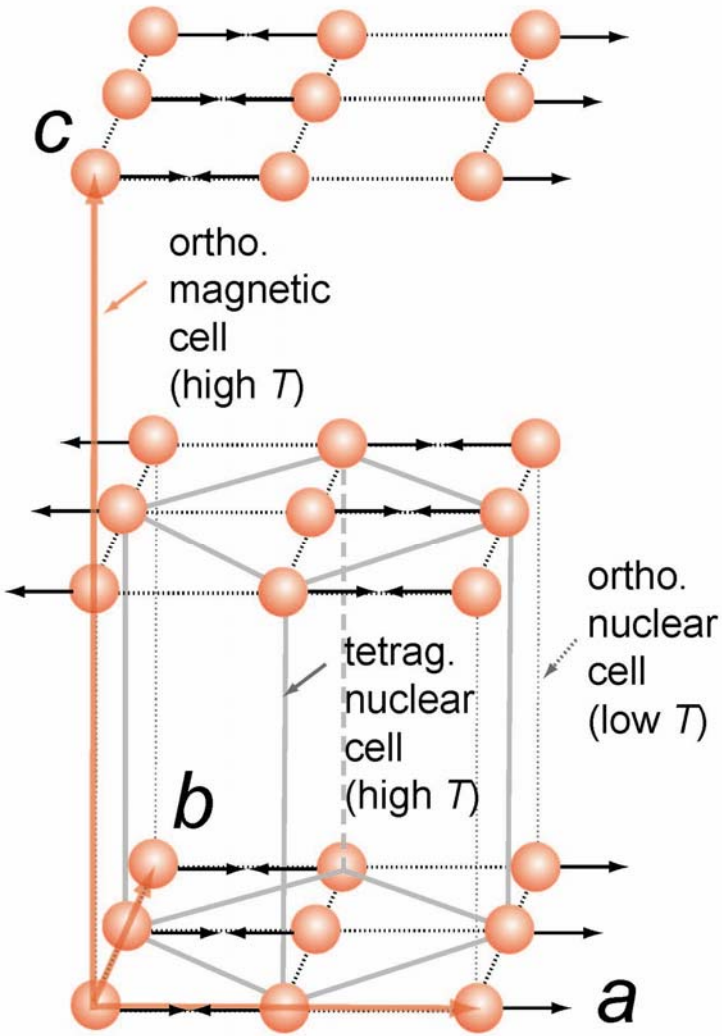

Magnetic Structure LaOFeAs

PSD
BT-7

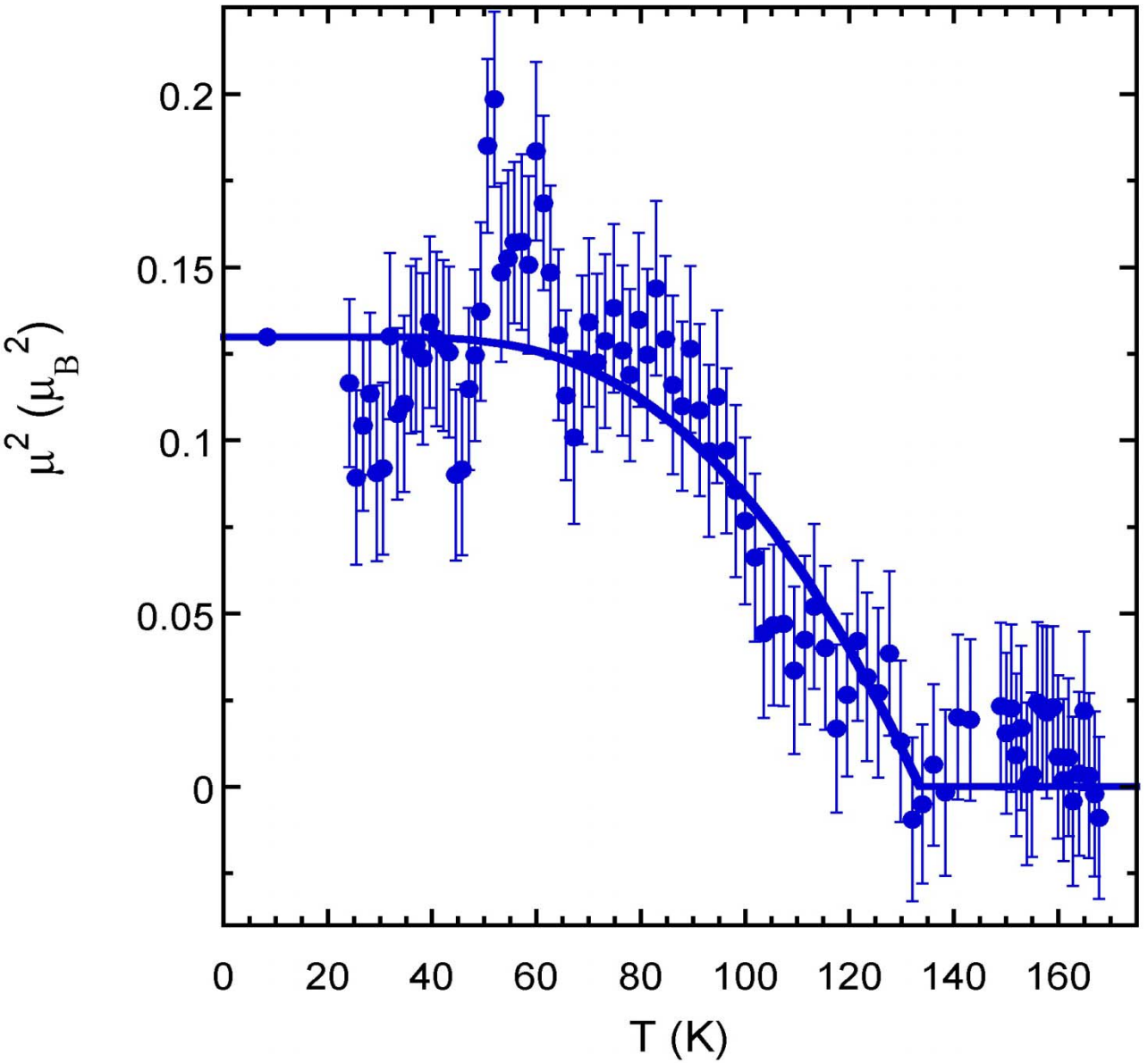

NdOFeAs Structure

PSD
BT-7

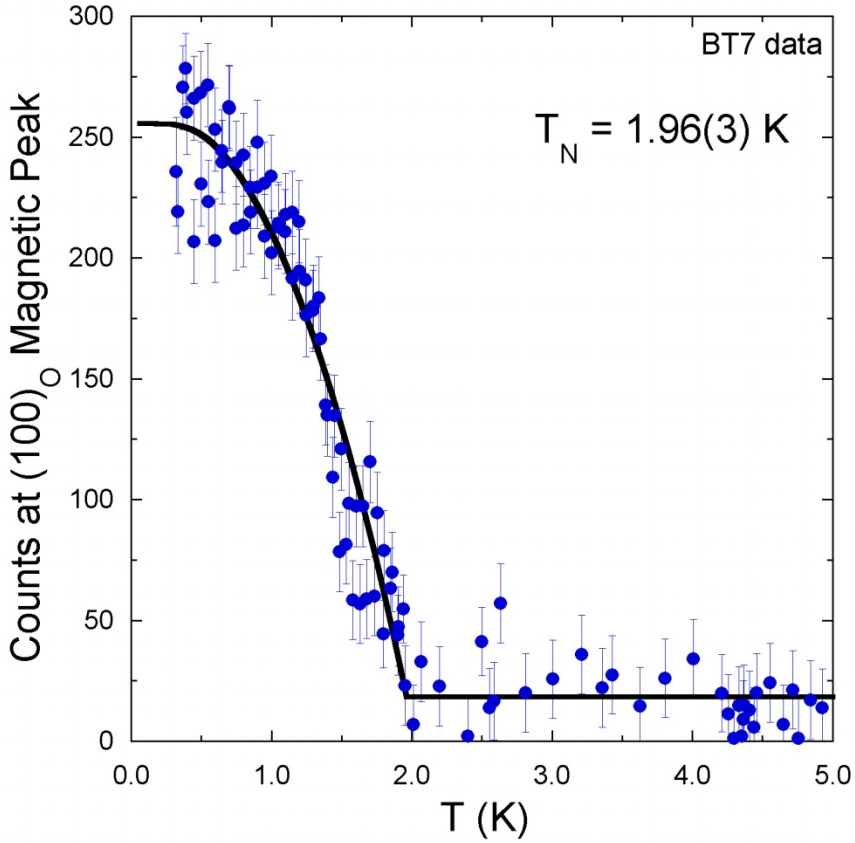

Polarized Beam

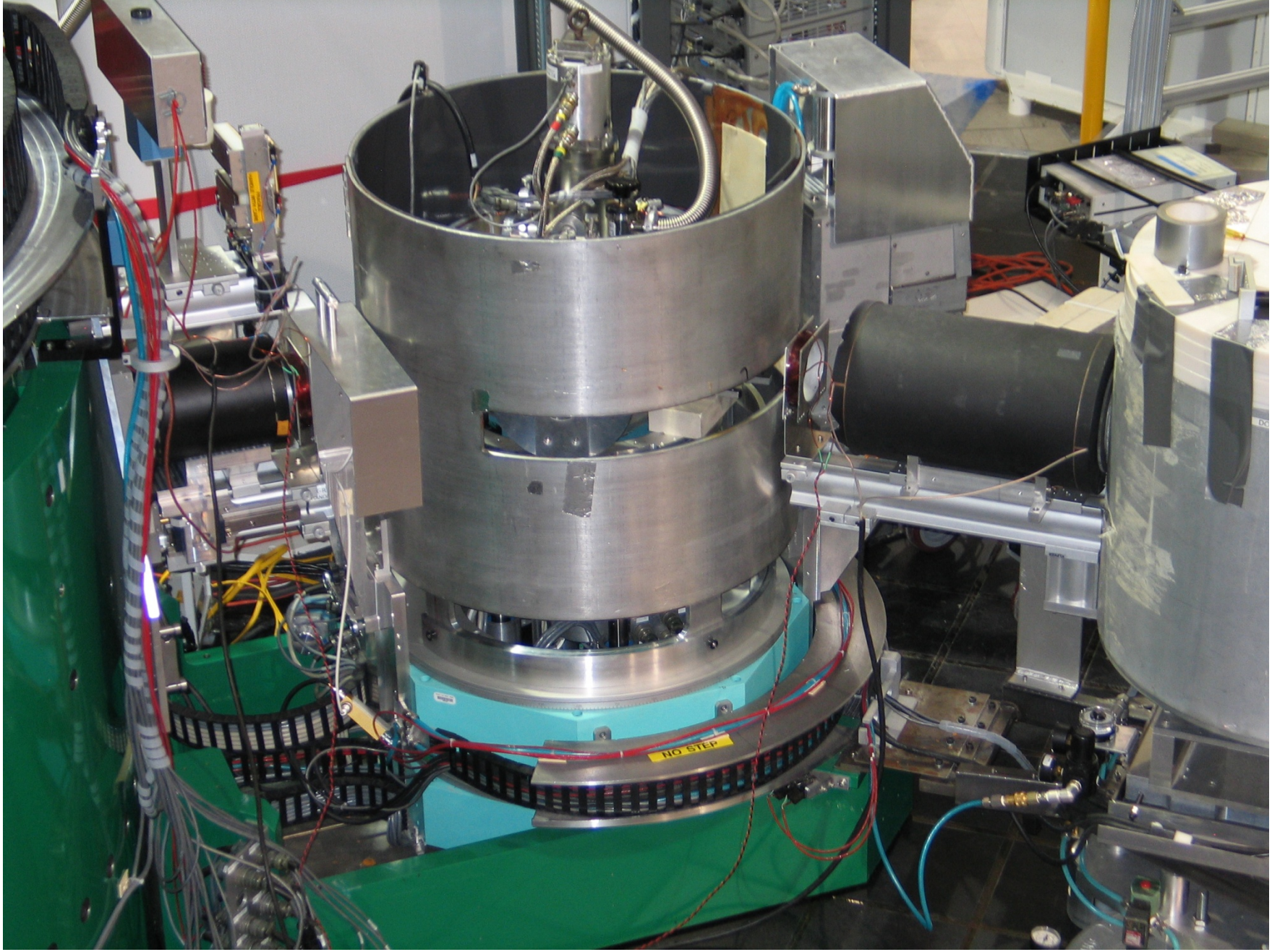
NO STEP

NdOFeAs

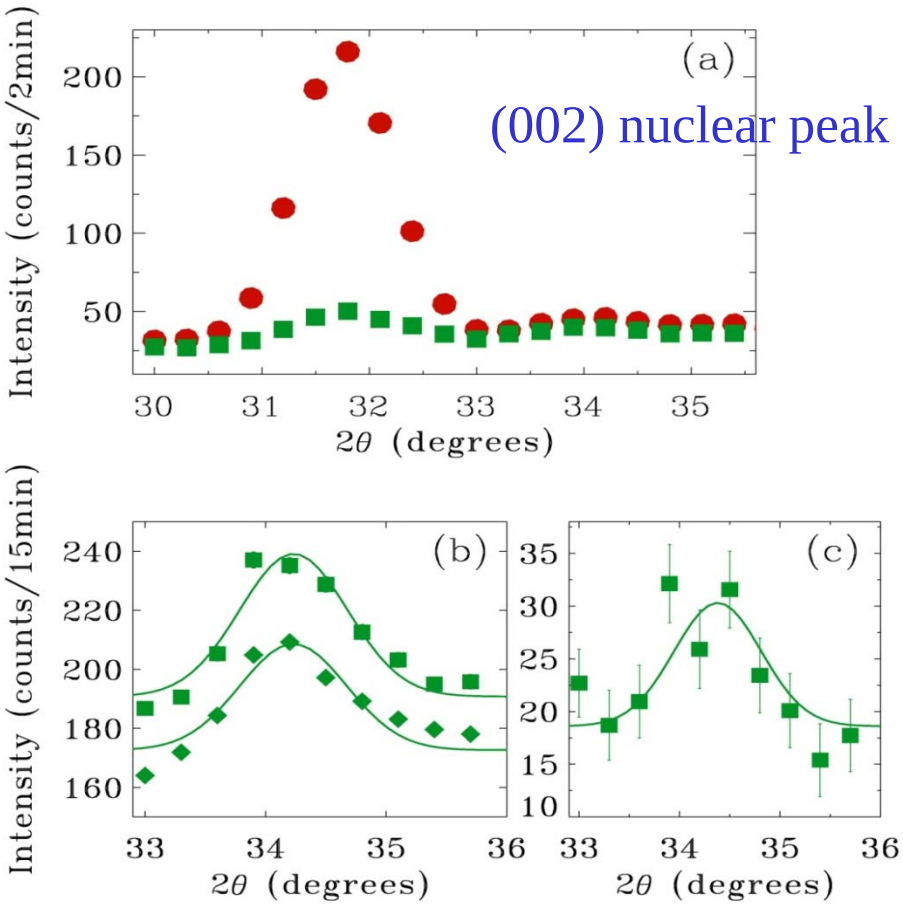

(002) nuclear peak

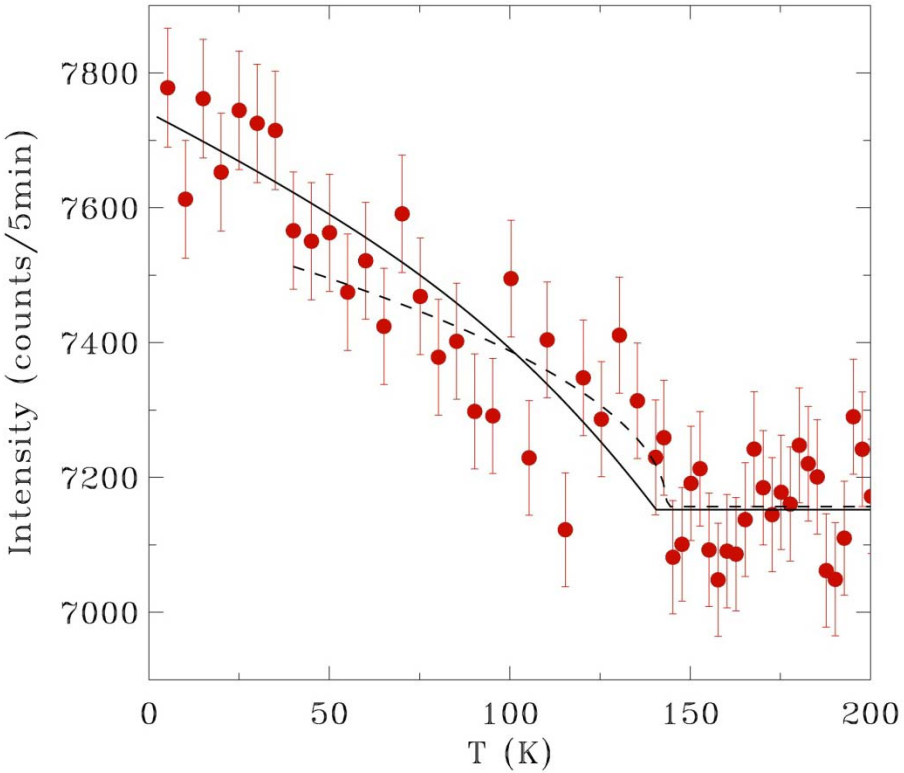

Polarized Beam (**P||Q** (squares) and **P⊥Q** (diamonds))

Spin Waves In $SrFe_2As_2$

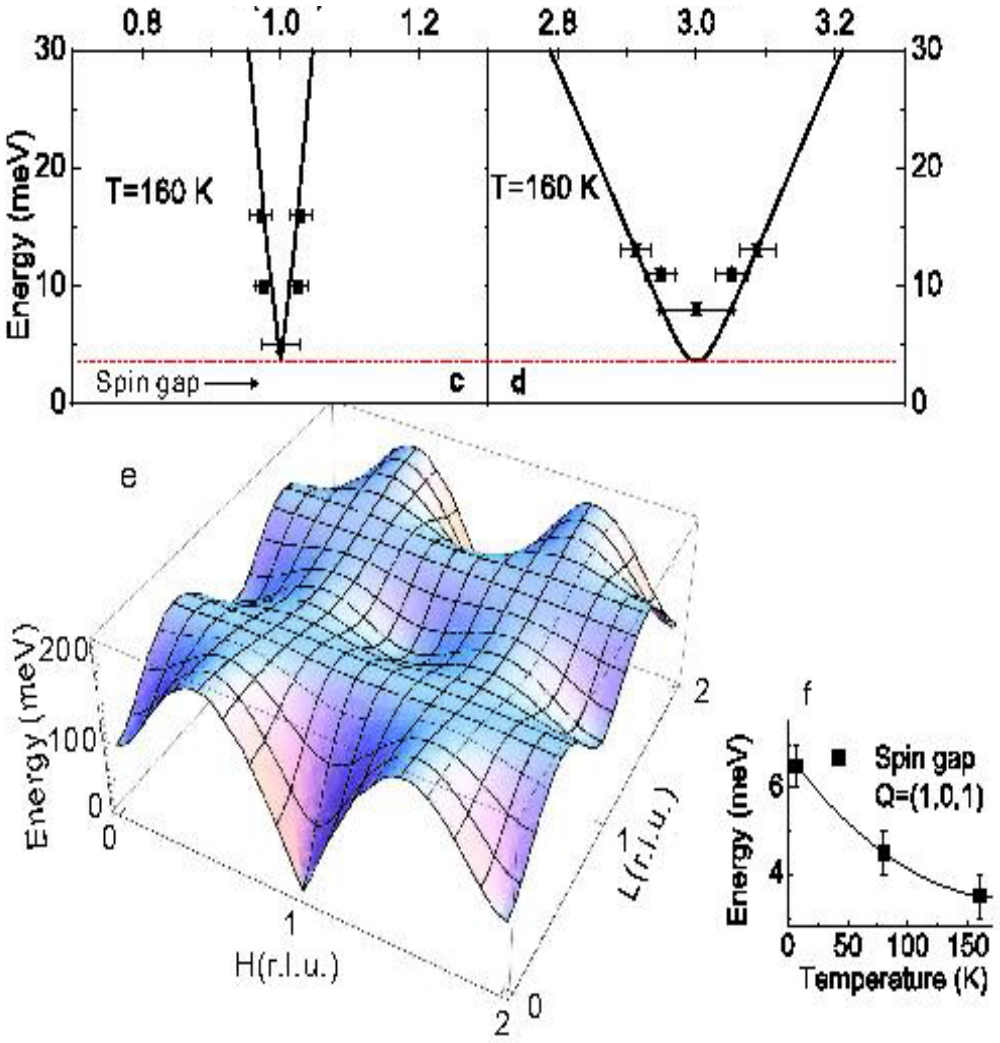

Jun Zhao, Dao-Xin Yao, S. Li, Tao Hong, Y. Chen, S. Chang, W. Ratcliff II, J. W. Lynn, H. A. Mook, G. F. Chen, J. L. Luo, N. L. Wang, E. W. Carlson, J. Hu, and P. Dai,

Phys. Rev. Lett. **101**, 167203 (2008).

Spin Excitations In Superconducting $BaFe_{1.9}Ni_{0.1}As_2$

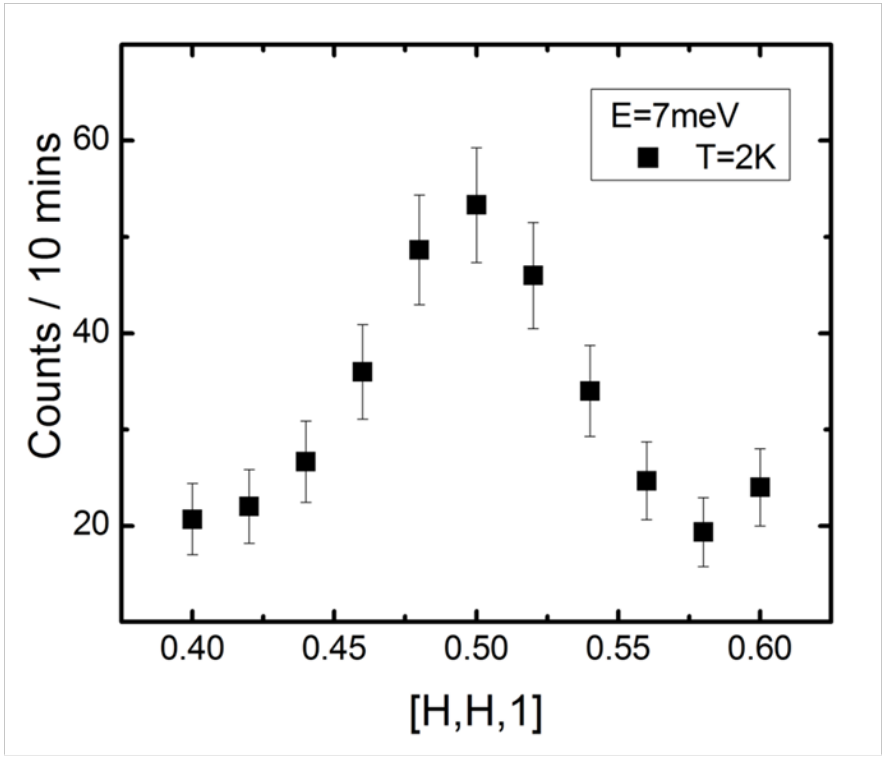

Resonance Energy

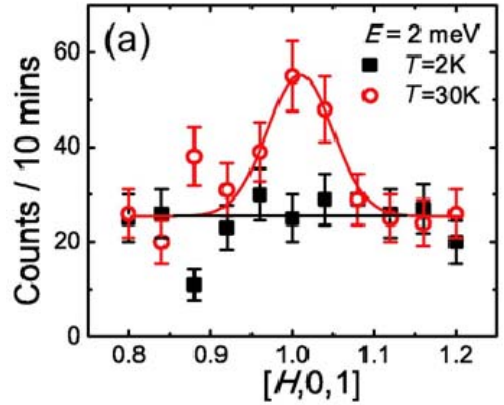

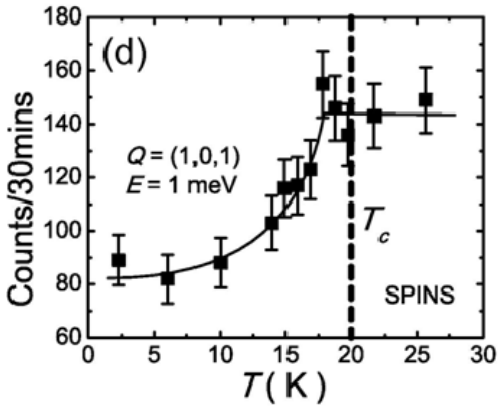

Spin Gap

S. Li, Y. Chen, S. Chang, J. W. Lynn, L. Li, Y. Luo, G. Cao, Z. Xu, P. Dai, Phys. Rev. B 79, 174527 (2009).

Magnetism in Hexagonal Ferroelectric $HoMnO_3$

Ferroelectric at 875 K (Ho sublattice)
Magnetic at 72 K (Mn)
Magnetic at 8 K (Ho)

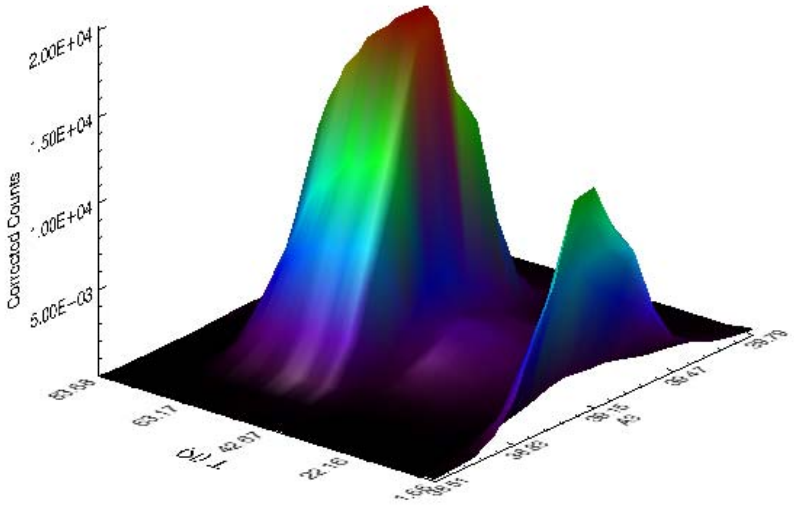

O. P. Vajk, M. Kenzelmann, J. W. Lynn, S. B. Kim and S.-W. Cheong, Phys. Rev. Lett. **94**, 087601 (2005);

J. Appl. Phys. **99**, 08R301 (2006)

$HoMnO_3$

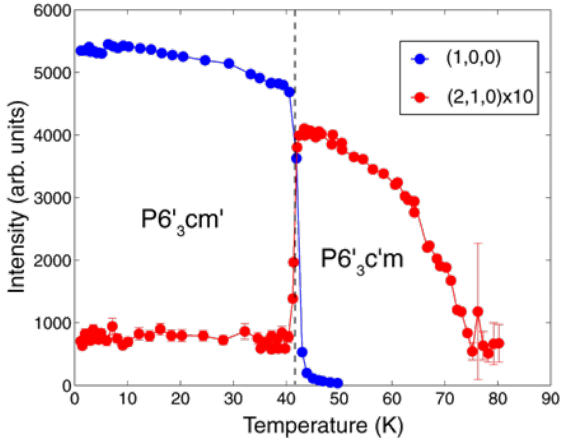
(1,0,0)
(2,1,0)x10
P6'3cm'
P6'3c'm
Intensity (arb. units)
Temperature (K)

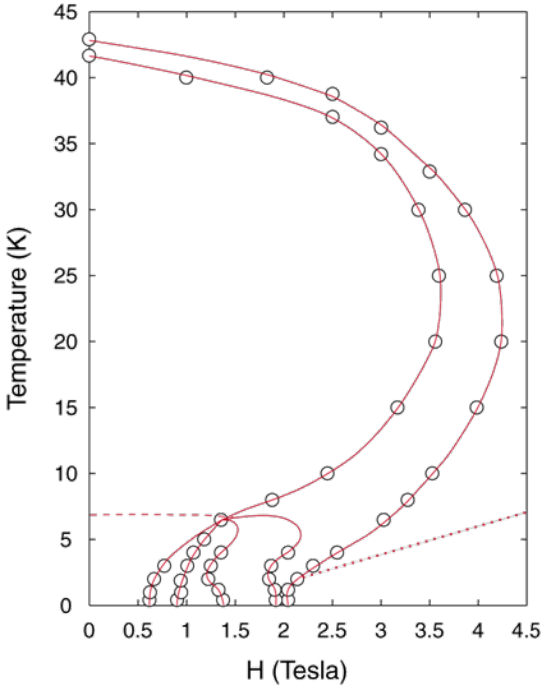
Temperature (K)
H (Tesla)

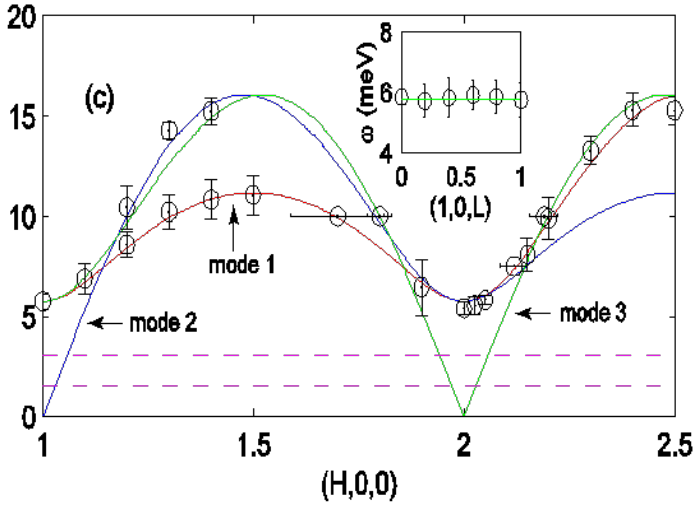
(c)
mode 1
mode 2
mode 3
ω (meV)
(1,0,L)
(H,0,0)

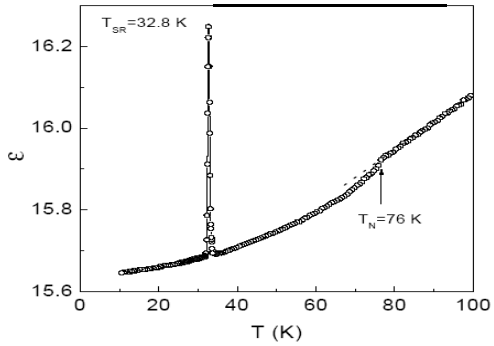
T_SR=32.8 K
T_N=76 K
ε
T (K)

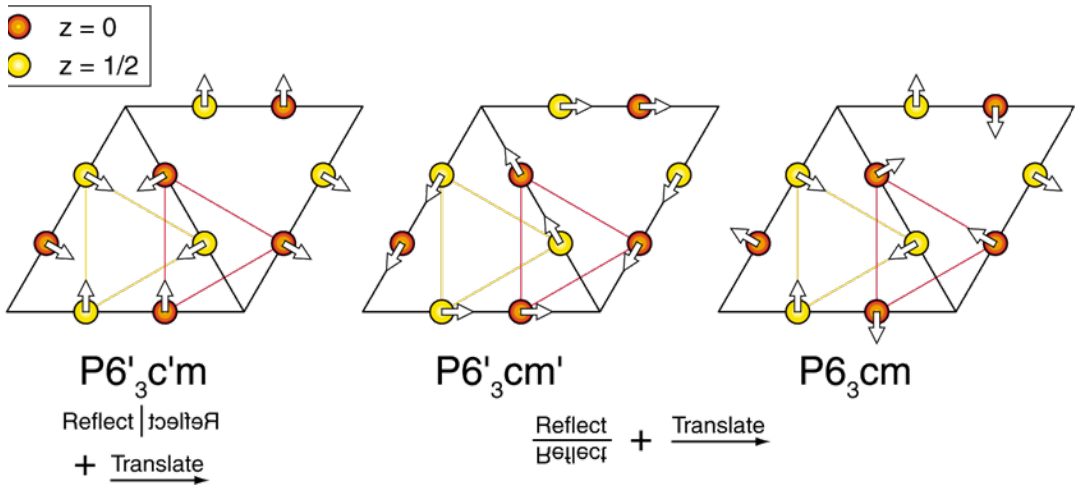
z = 0
z = 1/2
P6'3c'm
Reflect
Translate
P6'3cm'
Reflect
Translate
P63cm

2-Dimensional Spin-wave Dispersion

T = 20 K

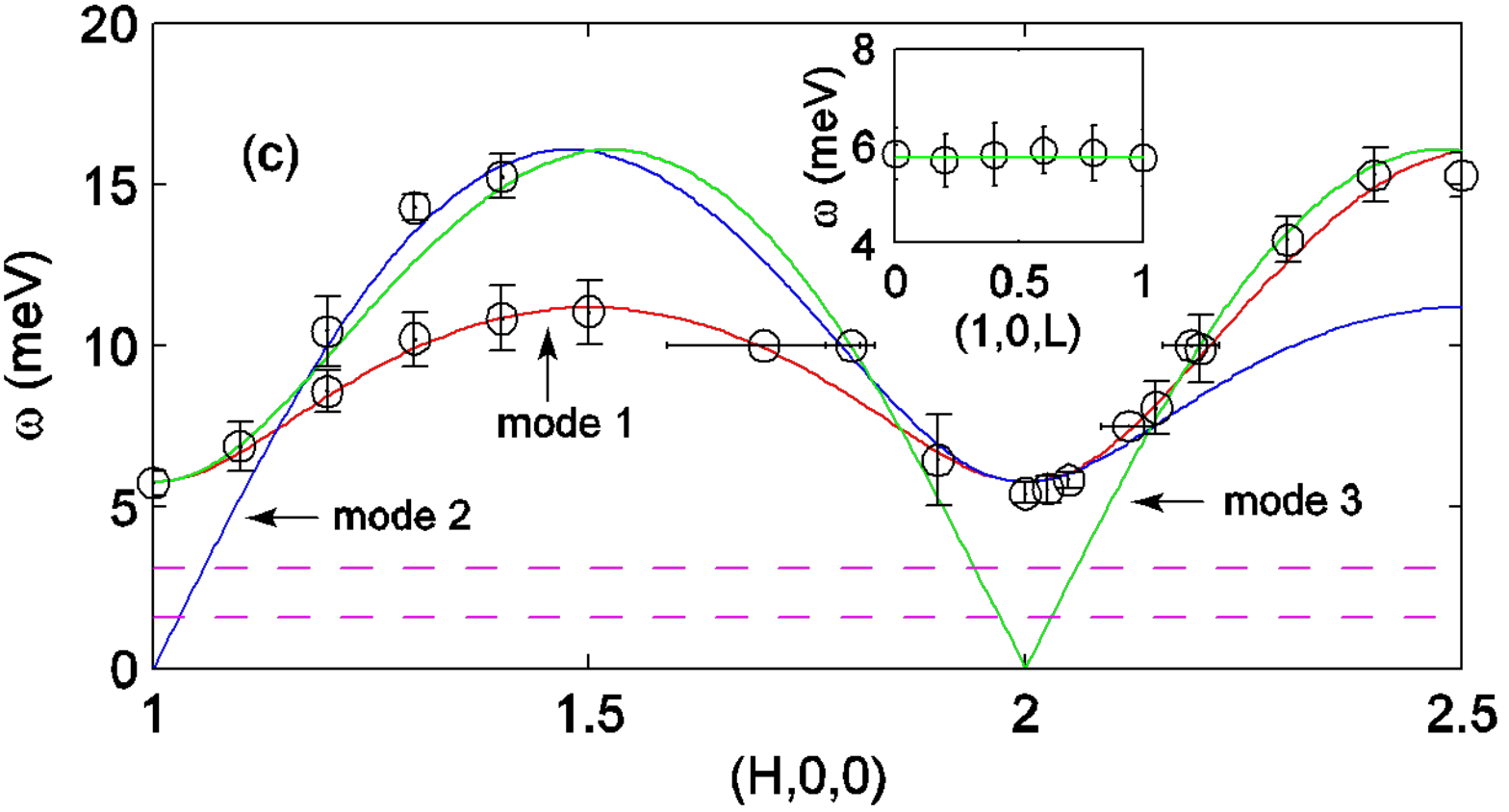

$$H = J \sum_{\langle i,j \rangle} \mathbf{S}_i \cdot \mathbf{S}_j + D \sum_i S_i^z S_i^z,$$

J=2.44 meV

D=0.38 meV

$Ni_3V_2O_8$ Multiferroic

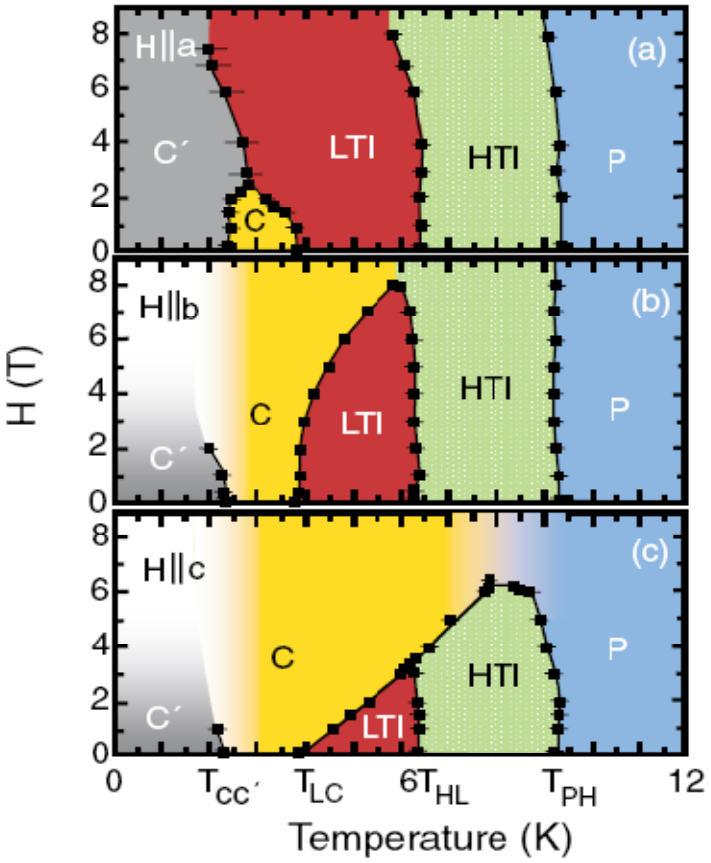

FIG. 2 (color). Phase diagram for NVO as a function of temperature and magnetic field applied along the three principal crystallographic directions. For **H** || **c** no true phase boundary separates the P and C phases. White areas were not probed.

G. Lawes, M. Kenzelmann, N. Rogado, K. H. Kim, G. A. Jorge, R. J. Cava, A. Aharony, E. Entin-Wohlman, A. B. Harris, T. Yildirim, Q. Huang, S. Park, C. Broholm, and A. P. Ramirez, Phys. Rev. Lett. **93**, 247201 (2004).

$Ni_3V_2O_8$ Multiferroic

Polarized Beam

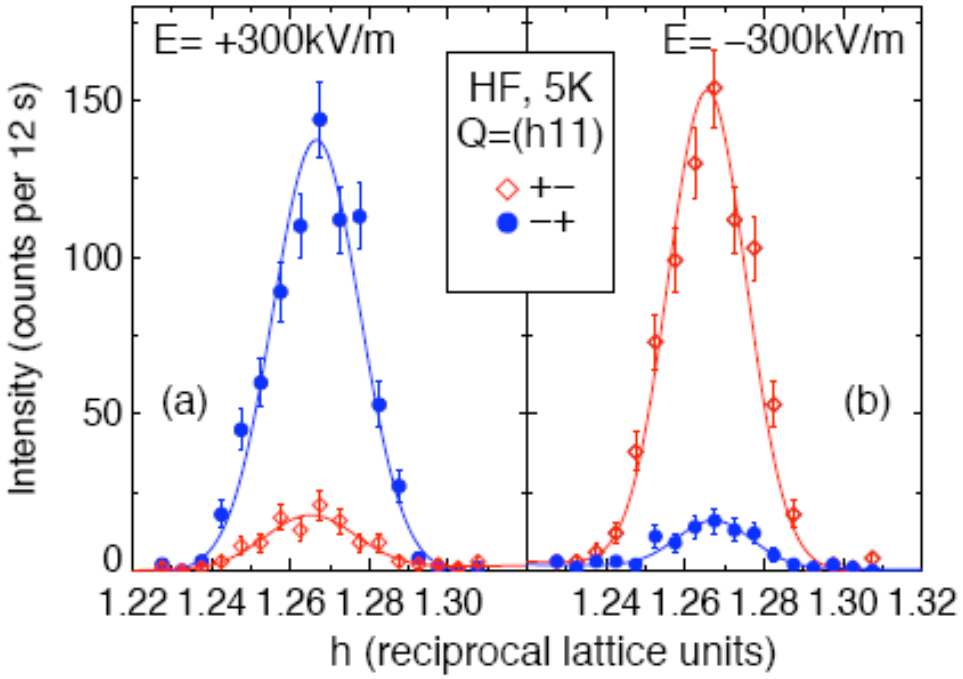

Coupled Magnetic and Ferroelectric Domains in Multiferroic $Ni_3V_2O_8$, Coupled Magnetic and Ferroelectric Domains in Multiferroic $Ni_3V_2O_8$, I. Cabrera,M. Kenzelmann, G. Lawes, Y. Chen, W. C. Chen, R. Erwin, T. R. Gentile, J. Leao, J. W. Lynn, N. Rogado, R. J. Cava, and C. Broholm, Phys. Rev. Lett. **103**, 087201 (2009).

$LiMnPO_4$ Multiferroic

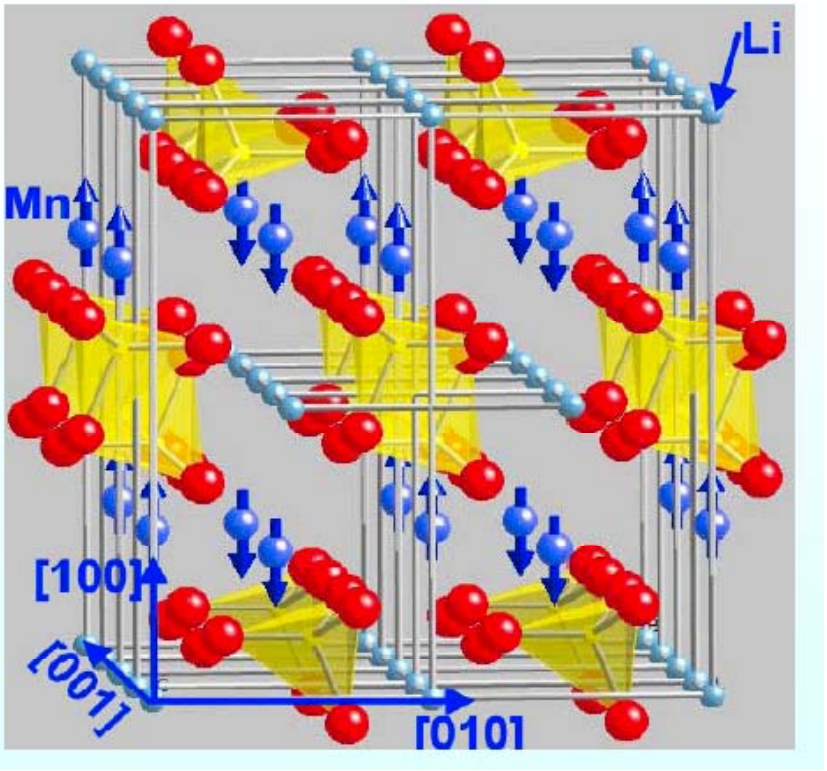

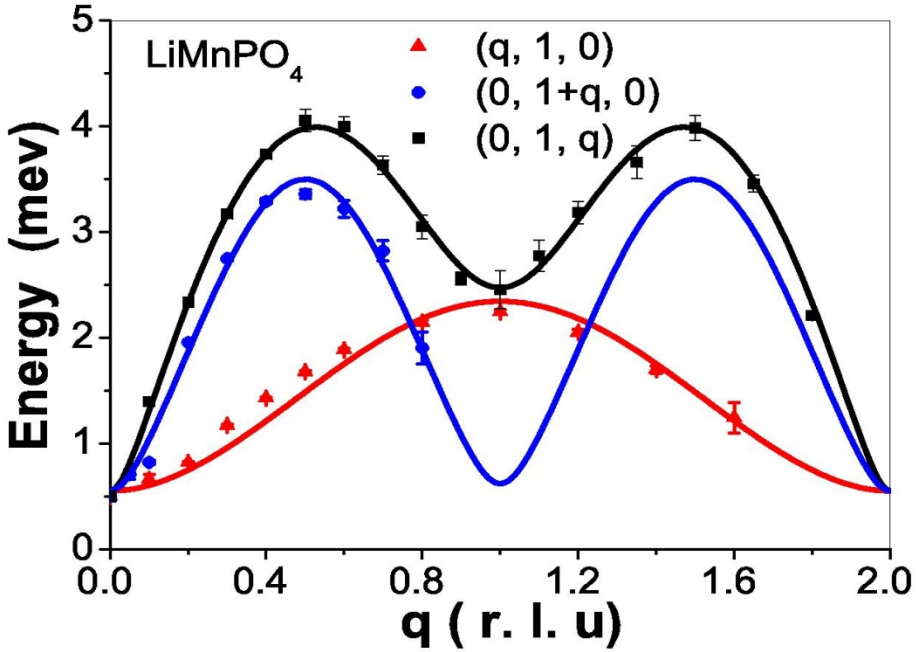

	S	J_1	J_2	J_3	J_4	J_5	D_x	D_y	D_z	J_3/J_1
$LiMnPO_4$	2.5	0.49(03)		-0.075	0.021		-0.29			

$T_N = 33.7$ K

Future TAS Instrumentation

- BT-7 Thermal Triple Axis—Next Steps
  - Ge(311) monochromator [replace Cu(220)]
  - New PSD (two dimensional)
  - ✓High Field Magnet accommodation

- *MACS*
- *BT-9⇒BT-1*
- *SPINS modernization*
- *Zero-field Spin Echo*